International Journal of Impact Engineering 170 (2022) 104372

Contents lists available at ScienceDirect

International Journal of Impact Engineering

journal homepage: www.elsevier.com/locate/ijimpeng

Simulation of PVB-glass adhesion and its influence on the blast protection properties of laminated safety glass

D. Aggromito [a,*], L. Pascoe [b], J. Klimenko [b], J. Farley [b], M. Tatarsky [c], W. Wholey [c]

[a] Arup US, 560 Mission St, Suite 700, San Francisco, CA 94105, USA
[b] Arup Australia, Sky Park, One Melbourne Quarter, 699 Collins St, Docklands, VIC, 3008, Australia
[c] Arup US, 77 Water St, New York, NY 10005, USA

ARTICLE INFO

Keywords:
Blast
Laminated Glass
Delamination
Viscoelasticity
Adhesion

ABSTRACT

Laminated safety glass (LSG) is frequently used to protect building occupants from hazards associated with explosions. The benefits of using LSG for blast protection have been well researched, and it is now commonly adopted within the construction industry to reduce hazards. The viscoelastic behaviour of the polyvinyl butyral (PVB) interlayer incorporated within the glass make-up allows designers to utilise the post-fracture capacity of an otherwise brittle material (glass). While glass fragments remain bonded to the PVB interlayer, the flexible membrane can undergo large deformations, resisting higher blast loads compared to monolithic glass panels. In order to adequately quantify the protective benefit of LSG, a thorough understanding of the post-fracture mechanical behaviour is required.

This study seeks to explore the influence of adhesion at the glass-PVB interface on the behaviour of LSG panels subjected to blast loads. It will draw on findings from previous material testing, previous full-scale blast testing data and numerical simulation to develop a validated numerical model of glass-PVB adhesion that is suitable for engineering applications. Once the numerical model is validated, the influence of glass-PVB adhesion levels will be explored. The findings are intended to draw attention to the influence of glass-PVB adhesion in the design of LSG systems for blast protection.

1. Introduction

Laminated glass (also known as Laminated Safety Glass or LSG) incorporating a Polyvinyl Butyral (PVB) interlayer is a composite material that combines the durable and visually permeable properties of glass with the benefits of a ductile viscoelastic polymer. LSG is extensively used in both the automotive industry and in architectural applications due to its enhanced impact resistance and ability to retain the sharp glass fragments from an otherwise brittle failure mode.

Within the field of blast resistant protective design, LSG is often used to meet two overarching objectives of blast protection: maintaining the building envelope and minimising flying debris [1]. When suitably captured by its framing system, LSG can undergo large deflections following the fracture of the glass plies, limiting the ingress of the blast wave beyond the building envelope while also providing an adhesive surface to retain glass fragments, reducing fragmentation hazard.

The two primary components of LSG, glass and PVB, possess complex mechanical characteristics. When combined to form a composite material, such as LSG, these characteristics result in a non-linear material. Previous studies have identified that the protective performance of LSG is dependant on several factors; traditionally these have included the material thicknesses, glass heat-treatment, pane geometry, and support conditions. These factors were well understood in the 1990s and included in publications such as the Glazing Hazard Guide [2]. Such research was used to develop engineering models to predict the protective performance of LSG systems [3]. Subsequently, LSG's mechanical properties and performance under blast loads were investigated in detail by others [4,5]. More recently, factors such as interlayer mechanical properties, temperature, and adhesion level, the bond between the interlayer and the glass itself have been identified as influencing the protective performance of LSG [5,6]. Engineering models capable of capturing the influence of adhesion on LSG's mechanical properties are recognised and well-studied in low to moderate strain rate environments (e.g. automotive windshields [7]). However, assessment of the influence of adhesion at the higher strain rates associated with blast loading scenarios is limited to small scale samples [6] or qualitative findings [5].

* Corresponding author.
E-mail address: Daniel.Aggromito@arup.com (D. Aggromito).

https://doi.org/10.1016/j.ijimpeng.2022.104372
Received 30 September 2021; Received in revised form 8 August 2022; Accepted 27 August 2022
Available online 28 August 2022

The lack of engineering models to capture the influence of adhesion on behaviour of LSG under blast loads is a key gap. For Architectural applications, in the authors' experience, interlayer thickness and adhesion level tends to be driven by long term durability requirements, particularly to reduce the potential for flaws such as delamination. This leads to a preference for "high" adhesion interlayers in architectural applications. Owing to the high frequency of potential glazing defects compared to the instances of explosions in the public realm, it is considered likely that glazing suppliers will continue to adopt such "high" adhesion interlayers. Therefore, it is important that the potential influences of using such interlayers on the blast protective objectives described in [8] is quantified.

In this study, a numerical model of PVB and associated adhesion to glass has been developed in LS-Dyna and correlated with physical sample and full-scale blast test results sourced from literature. Simulations are undertaken on a full-sized glass pane subjected to blast loads. In these simulations, the level of adhesion at the glass-PVB interface is modified based upon published values for "high" and "low" adhesion. From these simulations, the authors will draw conclusions on the influence of glass-PVB adhesion on the protective behaviour of LSG systems.

Firstly, an interlayer material model representing PVB is proposed. This model is intended to capture the mechanical properties of PVB at the high strain rates ($10s^{-1}$ to $40s^{-1}$) associated with blast loading and correlated with existing tensile test data. This model is developed into an LS-Dyna material model which is applied to 3D hexahedral elements. Next, a method to represent the bond between the PVB and glass is proposed. This utilises cohesion elements to represent adhesion between the PVB and the glass layer elements. A series of simulations are then conducted to correlate against physical tests of PVB-glass adhesion presented in literature. Finally, the full-scale arrangement is compared to two physical blast tests to determine how adhesion effects the behaviour of the pane under a blast load.

2. LSG characterisation

LSG is a composite material made up of two parts; an interlayer, often PVB, and at least two glass plies either side of the interlayer. Common LSG applications use a single interlayer, however, specialist applications (e.g. attack or ballistic resistant glass) may utilise a multi-laminated construction. LSG is typically formed by placing the glass-PVB layup into an autoclave to allow chemical and mechanical bonds to form between the glass and interlayer. This bonding (referred to as adhesion for the remainder of this paper) has been demonstrated to influence the delamination behaviour of LSG under blast loading [6]. The process of autoclaving also cures the PVB interlayer, modifying its mechanical properties [4].

Common with many composite materials, LSG's physical response to blast loads is complex and highly variable. Characterising these elements is challenging and requires each of the individual parts to be quantified and investigated in detail. Historically, limitations in state of knowledge and analytical capacity have resulted in the use of "smeared" material formulations in finite element models to predict LSG protective behaviour under blast loads and the use of simplified single and multi-degree of freedom models [3,4].

PVB's mechanical response is strain-rate dependant, and it can undergo several lengths of extension before returning to its original state [6]. Multiple authors have completed physical testing of PVB samples over a range of strain rates. These experiments demonstrate that at low strain-rates, the PVB exhibits a visco-elastic response where it stretches to multiple times its initial length before returning to its original state without significant permanent deformation. At higher strain rates, PVB initially presents a stiff response that appears linear-elastic before displaying the aforementioned visco-elastic traits [4,9,10,11]. The ductility of PVB reduces as strain-rate increases [11]. Zhang et al. [11] completed a variety of low speed and high speed tests on PVB using a Split Hopkinson Pressure bar and found that as strain rate increases, PVB transitions into a bilinear viscoelastic material, increasing the pseudo yield stress from 3 MPa at a strain rate of $8s^{-1}$ to 20 MPa at $1360s^{-1}$. Studies into PVB response to thermal change also identify a high level of temperature dependency. At higher temperatures, material stiffness reduces with an accompanying increase in PVB's extension to failure [12]. Furthermore, PVB response is also affected by environmental conditional changes such as moisture ingress [13] and ultra-violet radiation [14]. Suwen et al. [15] conducted tensile tests of PVB at a range of high strain rates up to $300s^{-1}$ and 4 temperatures including −30 °C, −5 °C, 25 °C and 40 °C and found that the initial modulus of PVB is influenced by strain rate and temperature, with the initial modulus varying from 1 MPa to 600 MPa over the tested strain rate range and the temperature range. In this study, it was found that the initial modulus decreased with temperature.

The adhesion of PVB to glass is a combined chemical and mechanical bonding process [14]. Klock [16] notes that the adhesion between glass and PVB can be modified by adjusting the hydroxyl content of the PVB, the plasticiser content or through the addition of metallic salts. Rather than quoting numerical values for adhesion, PVB interlayer suppliers commonly denote adhesion into three categories, low (L), medium (M) and high (H) adhesion grades. The use of high adhesion interlayers is commonly recommended for heat treated glass to limit potential visual distortions and performance defects such as edge delamination [13]. It is also common for high levels of adhesion to be specified for applications in which higher residual load-bearing capacity is required, such as curtain wall façade arrangements used in high-rise buildings. In combination with the increased capacity to contain any glass fragments on its surface, high glass adhesion, in the authors' experience, is a desirable selection amongst façade designers due to its enhanced long-term durability.

The adhesion of glass to PVB has the potential to play a significant role in the capability of LSG to provide protection against blast effects. As identified by Hooper [5] and Samieian [6], when subject to tensile forces, samples of cracked LSG exhibited progressive delamination. Where this occurs, PVB delaminates from the glass fragments, increasing the available length of PVB within each crack zone. This allows for stresses within the PVB ligament to remain near constant while increasing the overall extent of PVB available to extend. As a result, significantly more energy is absorbed by the interlayer than would arise without such progressive delamination. The energy required to overcome adhesion itself was investigated by Del Linz [17]. While non-negligible, this energy is not significant in the total quantity of work done by an LSG pane subjected to blast loads.

Owing to this phenomenon, these studies indicate that PVB adhesion may also influence the protective design properties of LSG panes. At high levels of adhesion, the stress state required within the interlayer to overcome the increased adhesion can result in an increased level of strain in the PVB ligament as it bridges the gaps between the glass fragments during deformation [13]. The localisation of strain has the potential to cause tensile rupture of the PVB, particularly in thinner interlayers, reducing protective benefits. Conversely, lower adhesion has the potential to allow the glass fragments to delaminate at an increased rate to reduce localised strain. This increased delamination of the glass fragments may increase the fragmentation hazard, as glass detaches from the interlayer, defeating one of the objectives of the interlayer usage [18]. Note that Samieian [19] identified a similar behaviour where PVB temperature changes occur, however this phenomenon is not further addressed by the authors at this time and may be the subject of future works.

Additionally, LSG panes are often structurally bonded to their framing systems using adhesives, such as silicone, to improve their protective performance. A key parameter identified by Descamps et al. [20] is the edge reaction force arising from the glass pane. The behaviour of silicone joints for blast resistant design applications was characterised by Hooper [5]. From these it can be understood that variances

in adhesion and hence delamination and PVB stress state under blast loads may also influence the magnitude of edge reactions. Therefore, the level of adhesion between the interlayer and glass will directly influence the size and strength of silicone joints within a blast resistant glazing system.

As outlined above, research by others has worked to characterise elements of LSG systems. However, quantification of the effects of interlayer adhesion on LSG response to blast loads for engineering design applications remains a gap in existing knowledge.

3. Methods for measuring interlayer adhesion

Several methods have been developed to estimate interface adhesion for LSG composites including the: pummel test, compressive shear test, peel test, and through-cracked tensile test (TCT). These test methods are typically adopted for in-house quality control by interlayer manufacturers. Further methods such as boiling tests are also used as part of quality control and durability prediction but are not suitable to derive specific mechanical properties. Results from adhesion performance testing are found to have significant variations, suggesting this is dependant on the composition of the PVB, chosen test methodology, and test conditions. Depending on the test performed, other forms of energy loss may need to be considered prior to comparison [21].

Pummel testing (Fig. 1) of LSG involves repeated impacting of a representative sample with a 0.5 kg hammer at 1.25 cm intervals via specifically designed impacting rigs. The repeated fractures induce bulk fracture and delamination of glass shards. Testing can also be completed at reduced and elevated temperatures as required. Glass performance is then qualitatively compared to standardised impacted samples to determine the damage level on a scale of 0-10 [22].

Compression shear stress (CSS) testing (Fig. 2), as studied in detail by Jagota et al. [22], involves mounting a specimen sample in an assumed rigid rig at a 45° incline. Compressive loading is then applied to the rig to induce in-plane shear (mode II) between the glass panes and interlayers. As identified by Jogota et al. [22], the deformation of the test specimen under this loading is complex and the ability to determine the interfacial resistance is highly dependant on the failure mode induced.

Peel testing (Fig. 3), as studied by Palfrene et al. [23], involves the application of a (measured) tensile load to the PVB interlayer typically at an angle of 45° or 90° from the plane of the sample. This requires the preparation of a specific test sample due to the necessity for the removal of the 'top' layer of glass. Frequently, an aluminium foil layer is applied to act as a stiff backing which reduces longitudinal stretching of the interlayer. As defined in ISO 8510-1, sample temperature and environmental humility are controlled.

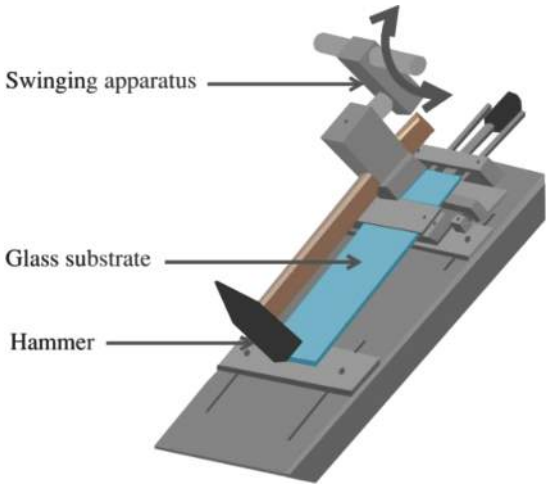

Fig. 1. Pummel Test Set-up.

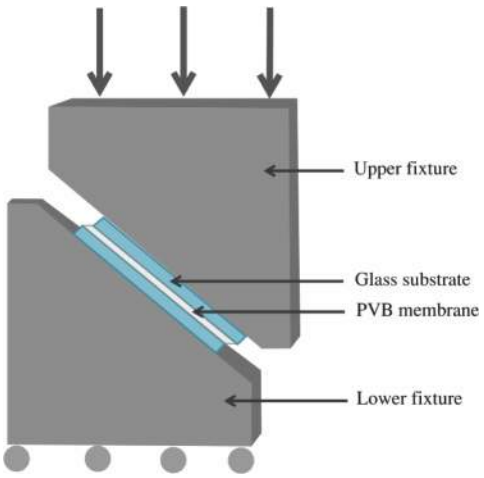

Fig. 2. Compression Shear Test Set-up.

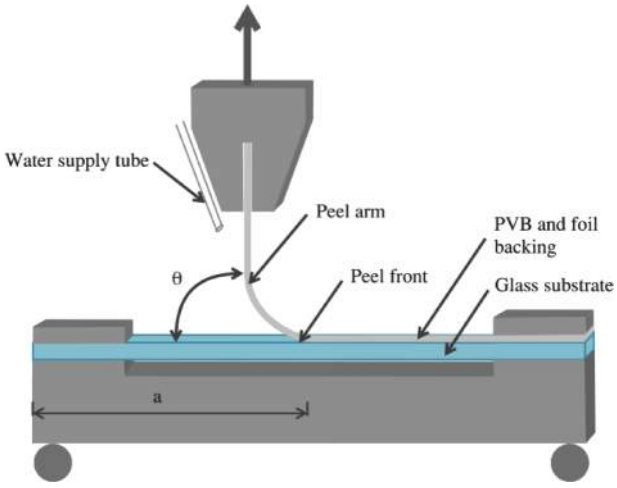

Fig. 3. Peel Test Set-up.

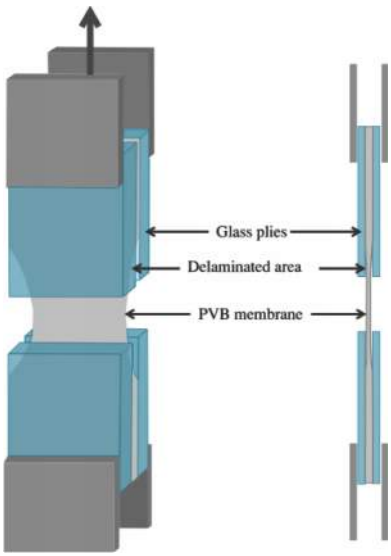

Fig. 4. Through-Cracked Tensile Test Set-up.

The through-cracked tensile (TCT) test subjects a pre-cracked laminated glass sample to a uniaxial tension load, as shown in Fig. 4. At the crack interface the PVB interlayer bridges the gap between the adjacent glass edges. During extension, the PVB interlayer progressively de-bonds around the glass edge until the interlayer has completely debonded from the glass or the PVB interlayer reaches its strain limit and ruptures. The force-displacement results from the TCT test can be used to determine the delamination energy by subtracting the strain energy from the total energy [6]. The through-cracked tensile test has advantages over the other test methods developed. Firstly, it is not as subjective as the Pummel test. Additionally, the data capture is simpler than the peel test as complications surrounding the bending of the peeling arm can be ignored because there is no physical bending of the interlayer. Finally, TCT tests most closely replicate the expected behaviour of glass panes subjected to blast loads. As such, TCT test data will form much of the data adopted for PVB and adhesion modelling described within this paper.

4. Experimental values for interlayer adhesion

Del Linz [24] proposed that PVB-glass adhesion be represented by a bi-linear traction separation curve where σ_max is the peak delamination stress, δ is displacement, K is traction stiffness and G is the area under the curve and the delamination energy (Fig. 5).

A review of literature was undertaken to investigate values for peak delamination stress (σ_max) and delamination energy (G) from physical / laboratory testing data. As illustrated in Table 1, the PVB adhesion properties vary substantially based on PVB thickness, PVB manufacturer, strain rate, and test methodology.

It can be observed that an increase in loading rate results in an increase in delamination energy. For a 1.52 mm PVB thickness, data from both Del Linz [24] and Samieian [6] indicate delamination energy rapidly increases with loading rate before reaching a plateau region of approximately 2500 J/m^2 to 3000 J/m^2 beyond an actuator velocity of 1000 mm/s.

Pelfrene [23] and Elziere [26] used a 0.76 mm PVB thickness and loading rates of 2.11 mm/s and 10 mm/s respectively to determine a delamination energy value for "low" adhesion. The authors note that the difference in values (452 J/m^2 and 69 J/m^2) may be attributed to Pelfrene [23] using the peel test method and Elziere [26] adopting the TCT test method. Data from Elziere [26] also indicate that for a given interlayer thickness and range of loading speeds (5 mm/s to 10 mm/s), changes from "low" to "medium" and "high" adhesion equate to an approximate doubling of the delamination energy (2.5 times from "low" to "medium" and 2.7 times from "medium" to "high"). Sha et al. [12] also conducted a variety of through cracked tensile tests with Saflex RB41 and provided peak delamination stress and delamination energy values for low, medium, and high adhesion at low strain rates. This demonstrated a 50% increase in delamination energy between low and medium adhesion and a 90% increase in delamination energy between medium and high adhesion.

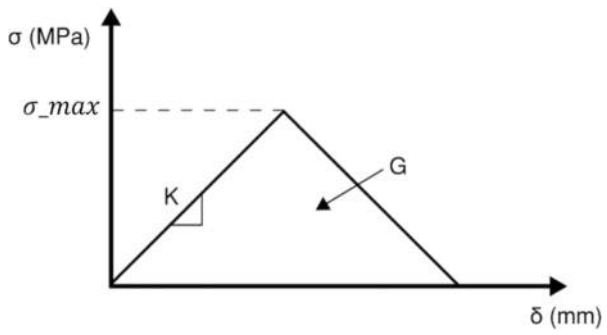

Fig. 5. Traction Separation Law used to describe adhesion of PVB interlayers.

While trends are observed in the data collected, it is clear from the range in values that determining a universally appropriate value for glass-PVB adhesion is challenging. Values vary according to test method, interlayer thickness, and loading rate. It is also noted that not all tests detail the temperature of testing, though it has been assumed that the average testing temperature was c. 20-25 °C (typical ambient room temperature). Owing to these factors, it is clear that additional data are required to validate any values chosen to represent specific glass-PVB adhesion in an engineering model.

5. Full scale blast testing

Full scale testing of window panes is typically conducted in two forms: open field tests or shock tubes, which can be driven by explosion or a combination high pressure gas and bursting diaphragm. Open field testing can be very costly, requiring a large open space and appropriate procedures for explosive material management. Shock tubes are closed test chambers designed to use a sudden release of a high-pressure gas to generate a shock front, simulating the effects of an explosion. Whilst significantly cheaper to operate, shock tubes can be limited in pressures and positive phase durations and, depending upon configuration, are also unable to create the damaging negative phase generated in open field explosions. ISO 16933 [28] and ISO 16934 [29] provide a useful overview of each test method and outline the level of instrumentation required.

Relevant data from full pane testing on LSG is limited, particularly as information security restrictions are frequently placed upon results. The quality of testing output was also found to vary based on the number of variables during a test and on the suitability of the data collection equipment. Frequently these tests are observational in nature with recorded performance based upon the number of fragments striking a witness panel [28].

In review of available blast testing data, two experiments were considered most relevant to this study. Kranzer [30] presents experimental results for 1.1 × 0.9 m laminated glass sheet exposed to Seismoplast PETN spherical charges in open-field blast experiments. Testing was completed with scaled distances of approximately 4 m/kg$^{1/3}$. The test samples were made of two annealed glass plies, each with a thickness of 3 mm and an interlayer of PVB with a thickness of 1.52 mm. Test specimens were constrained on all edges by clamping within a frame. The test results showed no failure of the interlayer under these conditions. The centre pane velocity and displacement were captured during the tests. These tests were not used to validate the engineering model within this study, as edge reactions were not measured, however, future work may consider these tests as additional validation. Hooper [5] performed a series of open-field blast experiments on 10 laminated glass samples each with a glass ply thickness of 3 mm and a PVB thickness of 1.52 mm. Digital image correlation (DIC) was used to measure the full rear-surface displacement of the pane, and strain gauges were used to measure the load that was transferred to the framing. In these tests it was found that the fracture patterns were characterized by densely cracked regions near the edges of the pane with lower density cracking in the centre of the pane. This was due to the initial deflection of the pane being nearly rigid body motion, which resulted in a distinctive "bathtub" shape of the fractured glass pane throughout its deflection time history. Such data indicates that strain rates across LSG panes are not uniform during blast events, a factor of key relevance in developing an engineering model of LSG.

6. Approach

To adequately explore the influence of glass-PVB adhesion on the performance of LSG systems intended for protection against the effects of blast, the authors propose a numerical model of LSG in LS-Dyna [31]. This model is intended to be suitable for engineering applications and the design of LSG and supporting systems. The approach will comprise:

Table 1
Review of Literature and the characterised adhesion properties for each test.

Reference	Test Method	Loading Speed (mm/s)	PVB Thickness (mm)	Adhesion Level	Delamination Stress (peak) σ_max (MPa)	Delamination Energy G (J/m^2)
Muralidhar et al. [25]	TCT	1	0.76	Not stated	3.228–5.354	283.98–929.14
Butchart al [9]	TCT	2.64E^{-2}	0.36	Not stated	Not stated	258
	TCT	2.64E^{-1}	0.36	Not stated	Not stated	660
Elziere, P [26]	TCT	10	0.76	Low	Not stated	69
	TCT	7	0.76	Medium	Not stated	170
	TCT	5.5	0.76	High	Not stated	460
Del Linz et al. [24]	TCT	10	1.52	Not stated	4.3	90
	TCT	100	1.52	Not stated	13.2	1275
	TCT	1E^3	1.52	Not stated	21.3	3000
	TCT	1E^4	1.52	Not stated	26.3	2750
Samieian et al. [6]	TCT	10	1.52	Not stated	2	322
	TCT	100	1.52	Not stated	2	2110
	TCT	1E^3	1.52	Not stated	2	2488
Pelfrene et al. [23]	Peel	2.117	0.76	Low	10	452
	Peel	2.117	0.76	Medium–	10	795
Sha et al. [12]	TCT	8.47E^{-3}	0.76	Low	1.22	104
	TCT	8.47E^{-3}	0.76	Medium	1.929	154
	TCT	8.47E^{-3}	0.76	High	1.929	295

the development of a PVB model, determination of appropriate numerical values to represent glass-PVB adhesion, comparison of the proposed glass-PVB composite with TCT and full-scale testing data obtained through literature, and simulation of a full-scale LSG pane with varying adhesion level.

7. PVB characterisation model

PVB characterisation has been studied in detail by multiple previous researchers [5,24]. At strain rates associated with blast loading (in excess of 10s^{-1}), PVB has been identified as non-linear (hyperelastic) in material response and highly dependant on a range of factors including temperature, humidity, strain-rate, thickness, and ultraviolet light (UV) exposure. An appropriate material model must therefore accommodate a range of material factors in an attempt to capture the potential range of response. In this study, a PVB model developed by Hooper [5] has been adopted and developed. The PVB interlayer was previously modelled using Abaqus finite element code. Hooper [5] conducted numerous tests at several different strain rates to characterise its strain rate dependency. Samieian et al. [6] and Del Linz et al. [17] used a three-term reduced polynomial and a two-term reduced polynomial strain potential, respectively, for the hyperplastic part of the curve. A Prony series was used to represent the viscoelastic aspects of the PVB. Results for both cases, however, required one set of constants to fit the curve for low strain rates (up to 8s^{-1}) and another set of constants to fit the curve for higher strain rates (above 8s^{-1} and up to 20s^{-1}). Del Linz et al. [17], attempted to implement an overall curve fit, but found that at lower rates a different curve fit was also required.

8. FEA model of PVB 'dogbone' sample

To replicate the tensile tests as described above, a model of the PVB 'dogbone' sample in LS-Dyna undergoing a tensile test was completed using LS-Dyna version 9.2. The PVB 'dogbone' sample assessed had a thickness of 0.76 mm with dimensions detailed in Fig. 6. The sample was fixed on one side with a boundary constraint, and on the opposite side it was pulled using a displacement correlating to the various strain rates that mimic the behaviour of the tensile tests conducted in experiments.. The PVB 'dogbone' sample was meshed using solid elements with 0.5 mm element size and a hexahedron 8 node solid element with an element formulation of −1 (fully integrated S/R solid elements). To represent the hyperelastic and viscoelastic parts of the PVB 'dogbone' sample MAT_77H was used.

MAT_77H uses a six-term polynomial to fit the hyper-elastic part of the material and is shown in Eq. (1).

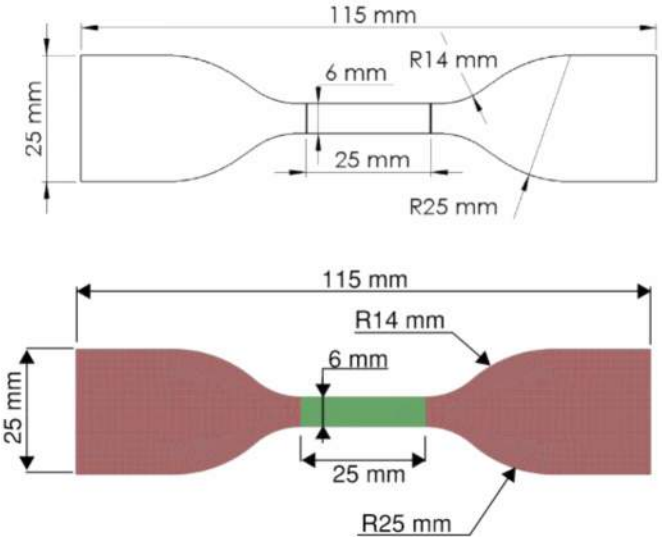

Fig. 6. Dog bone sample defined in Samieian et al. [6] with main dimensions and LS-Dyna model of dog bone sample with main dimensions.

$$W(J_1, J_2, J) = \sum_{p,q=0}^{n} C_{pq}(J_1 - 3)^p (J_2 - 3)^q + W_H(J) \quad (1)$$

Where W is the strain energy and is a function of the relative volume (J), C is the Cauchy-Green Tensor. This material model also has the option to include a Prony series which represents the viscoelastic parts of the material. It should be noted that the form of the Prony series in LS-Dyna [31] differs to the form in Abaqus. LS-Dyna (MAT_77H) uses a stress based Prony series, whereas Abaqus uses a constant based Prony series. The Prony series in LS-Dyna is detailed below:

$$g(t) = \alpha_0 + \sum_{m=1}^{N} \alpha_m e^{-\beta t} \quad (2)$$

Given by,

$$g(t) = \sum_{i=1}^{n} G_i^{-\beta_i t} \quad (3)$$

The material is effectively a Maxwell fluid which consists of dampers

and springs in series, G_i represents shear moduli, β_i are the decay constants [31] and α is a material parameter to be found. The material coefficients used to fit the material curves in the simulation are listed in Table 2 for the hyperelastic part and Table 3 for the viscoelastic part. Experimental results with model fits are shown in Fig. 8 and an image of the simulation is in Fig. 7.

As demonstrated in Fig. 8, the material fits well between 1 m/s and 5 m/s (actuator arm speed during TCT) and in particular correlates well in the strain regions typically seen by the PVB during the blast tests carried out by Del Linz et al. [17] and Hooper [5]. Deviation from tested values occurred at high strains for all loading rates (between 0.3 and 0.6 depending upon loading rate); above these values the simulation underpredicts material stress. This is a result of the PVB 'dogbone' sample undergoing large stretching, resulting in "hour glassing" of some of the solid elements. However, based on the simulations completed on TCT glass-PVB samples and full-size glass panes, the PVB strain does not typically achieve these strain values. Therefore, the magnitude of the negative effect on the validity of the simulation is assessed to be low.

While individual curve fits were found to demonstrate better correlation to test results, this introduces additional requirements to determine the expected strain rate within a glass pane prior to simulating the pane response. Additionally, strain rates are observed to vary spatially as well as temporally over a pane subjected to blast loads with some regions experiencing higher rates than others and strain rate varying throughout the pane's response. While the initial section of the curves underestimates the initial modulus of the PVB, the overall curve fit still demonstrates good agreement with the test data for the desired strain range, therefore the overall curve fit is used.

A mesh sensitivity study was completed to determine the influence of aspect element ratio with results shown in Fig. 9. The PVB thickness assessed in this study is 1.52 mm and the element size varies from 1 mm to 4 mm. As is demonstrated, altering the mesh density does not provide a substantial deviation from the test, however, as seen in Fig. 9, the larger mesh fails at a strain of 100% compared to 120% for 0.5 mm. To maintain efficient simulation run times, a 1 mm mesh density is used throughout the TCT Testing. The current PVB material model is unable to achieve a similar linear curve when the load is initially applied to the PVB. This is hypothesised to be a result of the PVB sample undergoing a slight tension load during the physical test in contrast to the simulation, in which the loading begins at 0 and ramps up to the desired rate.

Morison [4] noted that PVB exhibits differing loading and unloading characteristics. In particular, he observed a very low level of initial elastic strain recovery followed by long term recovery of PVB strain. The current LS-Dyna formulation does not account for this unloading phenomenon and is correlated with tension tests only. This behaviour has limited impact on the results of the studies presented within this paper.

9. TCT experimental data

The authors have reviewed test data provided by Hooper [5], Del Linz et al. [27] and Samieian et al. [6]. All three adopted the TCT test to investigate glass-PVB adhesion characteristics under high strain rates associated with a blast event ($10s^{-1}$-$40s^{-1}$). As such the TCT test method has been used for the simulation in LS-Dyna.

The TCT testing data collected by Hooper [5] included four laminated glass layups, each with two 3 mm plies of annealed glass and a single PVB interlayer of 0.38 mm, 0.76 mm, 1.52 mm or 2.28 mm thickness. The interlayer material tested was Saflex RB41 PVB produced by Solutia Inc. Laminated glass specimens were of nominal dimension 150 mm x 60 mm bonded with toughened methacrylate adhesive to 2 mm thick aluminium end tabs. Prior to testing, samples were fractured to simulate the conditions of the laminated glass observed in blast tests. Four different crack arrangements were made including: a single crack in both plies, 10 mm spaced cracks, 20 mm spaced cracks, and a randomly arrayed dense crack pattern. In total, 108 cracked glass samples were tested at displacement rates between 0.01 m/s-10 m/s and at a temperature of 20 °C. Similarly, Del Linz et al. [27] also conducted TCT tests of the same specimen size, glass thickness and interlayer properties for a single crack in both plies at the 0.01 m/s-10 m/s rates. Samieian et al. [6] adopted the same specimen size, glass thickness and interlayer thicknesses as Hooper [5] and Del Linz et al. [27], however, he tested 19 specimens at a loading rate of 1 m/s and varied the temperature range between 20 and 60 °C. The interlayer material used in these tests was manufactured by Everlam.

Table 2
Hyper-elastic material model parameters used for the PVB tensile test and through cracked tensile test.

Parameter	Overall Fit Value
C_{10} (MPa)	0.94
C_{01} (MPa)	2.06
C_{11} (MPa)	−0.23
C_{20} (MPa)	0.404
C_{02} (MPa)	0.0182
C_{30} (MPa)	−0.0063

Table 3
Prony series model parameters used for the PVB tensile test and through cracked tensile test.

β $(1/s)$	Overall fit G_i (MPa)
9080	684.5
10	3.0
11	4.78
2000	0.3

10. FEA model of through cracked tensile test

In this study, a through-cracked tension test model consisting of 3 parts has been created in LS-Dyna. The three parts are: the glass plies (3 mm thickness); cohesive elements (0.01 mm thickness) representing glass-PVB adhesion; and the PVB interlayer (1.52 mm thickness). Fig. 10 shows the geometry of the model with its dimensions indicated. The glass dimensions were 3 mm thick and 80 mm in length, split into two sections with each glass section having a total length of 39 mm. This test represents a single cracked glass specimen. Glass is simulated using a simple elastic material to reduce its influence on the adhesion. A consistent solid mesh with 8 node HEXA elements is used throughout the model with an aspect ratio of approximately 1:1 and a mesh size of 1 mm. The cohesive elements are meshed with an 8 noded 4 point cohesive element. To accurately represent the cohesive element delamination behaviour, a material that utilises a bilinear traction separation law for both the tangential and normal directions is used. A representation of the traction separation law is shown in Fig. 5. The PVB interlayer uses the material properties in Tables 2 and 3. The parameters used in the through cracked tensile test are summarised in Table 4.

The through cracked tensile test is pulled at 1 m/s to simulate the tensile tests described in the section above. A parametric study was completed varying adhesion parameters, principally peak delamination stress (σ_max) and delamination energy (G) based on values provided in Table 1.

Fig. 11 compares the engineering model to the physical test. Increasing σ_max led to a more representative shape of the output (early peak dropping sharply to a "plateau value") when compared to the test results. However, throughout the parametric study, it was not possible to replicate the rapid drop in observed peak tensile force to the steady state plateau level. The authors propose that this is attributed to the force required to initiate delamination being larger than that required to maintain a delamination front. In this respect, there are similarities with mechanical fracture mechanisms. This hypothesis is supported by Samieian et al. [6] who proposed that the bond fracture toughness is loading rate dependant, up to a limit of $20s^{-1}$, and that any further

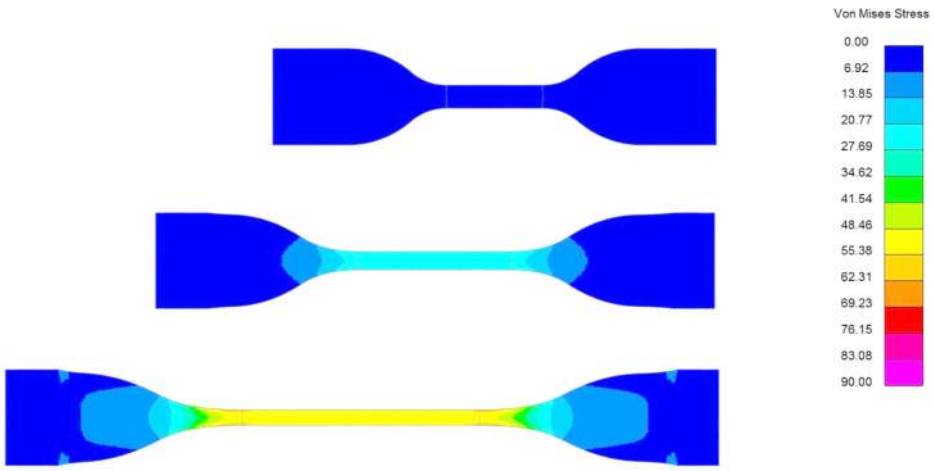

Fig. 7. Simulation of the 'Dogbone' Sample at 1 m/s (actuator arm speed) at a strain of 50% and 100%.

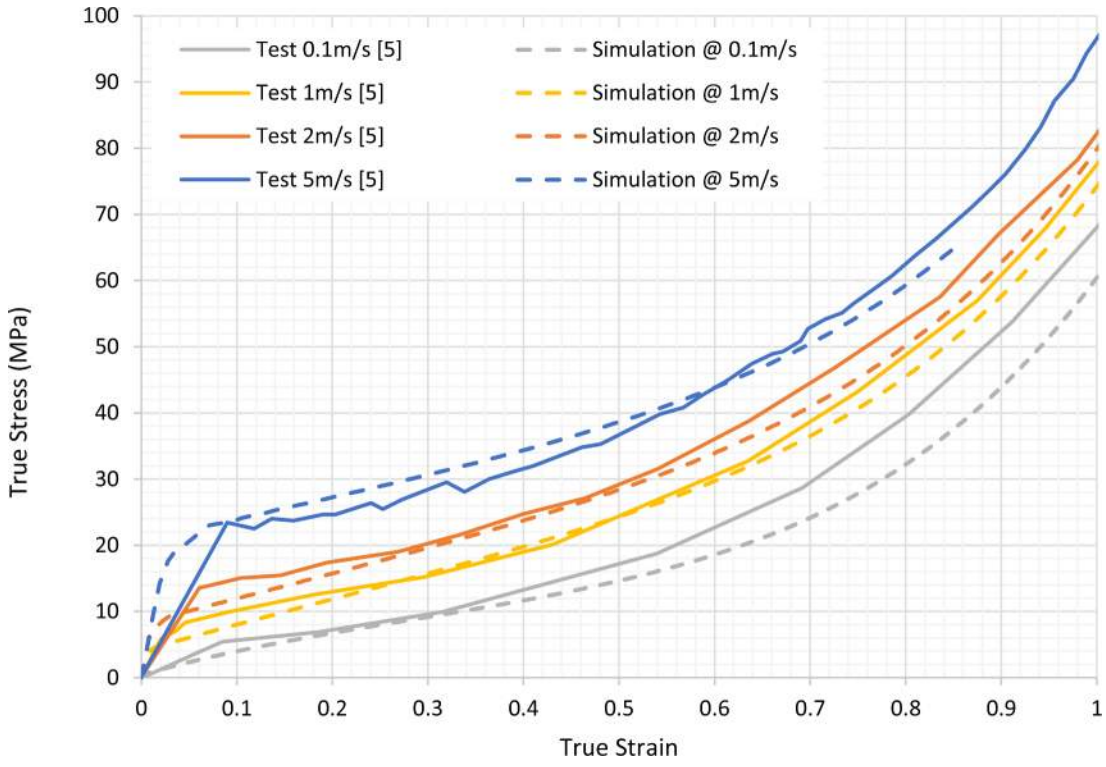

Fig. 8. PVB Tensile Test at Different Strain Rates (Overall Model Fit).

increase in loading rate did not result in a change in facture toughness. In the peeling of flexible laminates, Samieian et al. [6] stated that the fracture toughness is a factor of the local plastic or viscoelastic energy dissipation in the zone ahead of the peeling front. As can be observed later, the additional energy absorbed by the simulated interlayer is negligible and the forces (required to generate pane edge reactions) are consistent with tested values.

Previous testing undertaken [6,27,5] illustrates that the observed response of TCT samples was largely bilinear with initial elastic extension of the PVB within cracks transitioning to steady state delamination. This results in a force plateau being observed. As demonstrated in Fig. 11, results for force plateau in the simulation show good comparison to experimental results of Hooper [5], Del Linz et al. [27] Samieian et al. [6] at a rate of 1 m/s. Simulation results show a similar peak force, though the return to the plateau force is noted to be more gradual compared to experimental data. The variation between work done in the simulation and in the experiment (for up to 20 mm elongation) is less than 5% as summarised in Table 5. The tests were completed using an interlayer with a medium adhesion grade.

11. Full scale blast test simulation

Following determination of appropriate adhesion properties and comparison against the single crack TCT tests, the proposed PVB and adhesion material characterisation is compared to full scale blast test data. The purpose of this comparison is twofold. Firstly, it confirms the suitability of the derived parameters for the range of strain rates that a full pane would experience ($10s^{1}$-$40s^{-1}$ based on the PVB and adhesion correlation) and secondly, it determines whether the proposed model can predict reaction forces and failure modes associated with adhesion/

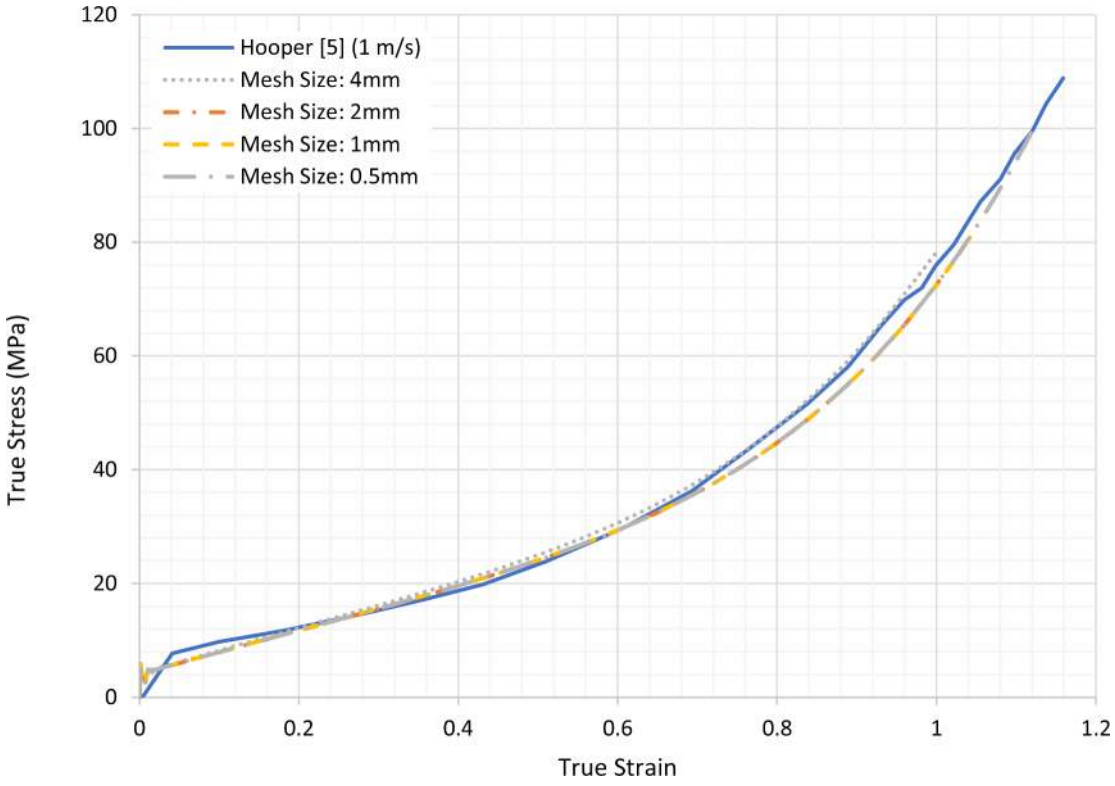

Fig. 9. Mesh Sensitivity Study at 1 m/s.

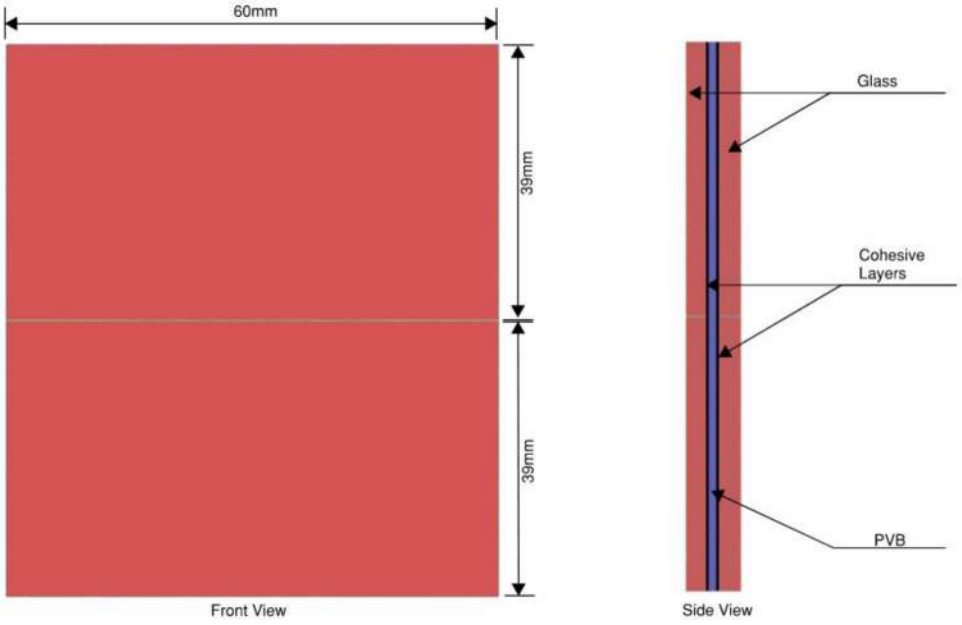

Fig. 10. Main dimensions and features of the single crack delamination models. Front and Side View.

Table 4
Summary of the materials employed in FEA models for the Through Cracked Tensile Test.

Material	Model Type	Material model	Summary of Parameters
Glass	Linear Elastic	MAT_1 ELASTIC	$E = 70$ GPa, ρ=2500 kg/m^3, ν=0.22
PVB	Hyperelastic with Viscoelastic Constants with a 6 term Prony series	MAT_77H HYPERELASTIC RUBBER	Refer to Table 2 and Table 3
Cohesive Elements	Bi-Linear Traction Separation	MAT_186 COHESIVE_GENERAL	$\sigma_{-max} = 1.8MPa,\ G = 3000\ J/m^2, K = 5.4E+09$

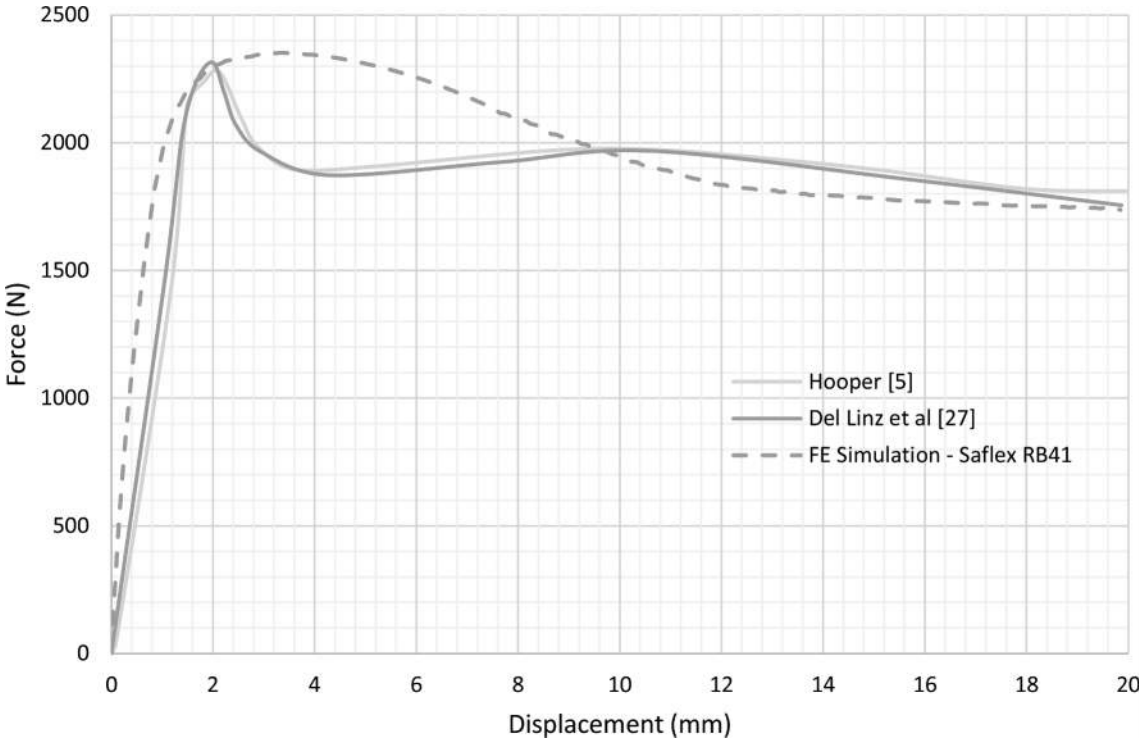

Fig. 11. Comparison of the FE model to the Through Cracked Tensile Tests.

Table 5
Comparison of Peak Force and Energy between the 3 tests and the engineering model.

	Del Linz et al. [27]	Samieian [6]	Hooper [5]	Engineering Model
Peak Force (kN)	2.31	1.94	2.28	2.35
Work Done (kN-mm)	36.67	32.8	37.02	38.7

delamination.

For this comparison, tests conducted by Hooper [5] have been used. Hooper carried out a series of full-scale, open-field blast tests adopting laminated glass with a PVB interlayer for a range of charge sizes (15-500 kg TNT equivalent) and standoff distances (10-30 m). Panes of 1.2 m by 1.5 m were supported along all four edges using structural silicone bonded to a steel subframe. For each test, an explosive charge was detonated in front of the test cubicle. High-speed 3D digital image correlation was used to track the rear-surface position of the window, allow the time histories for deflection, deformed shape, velocity, strain, and

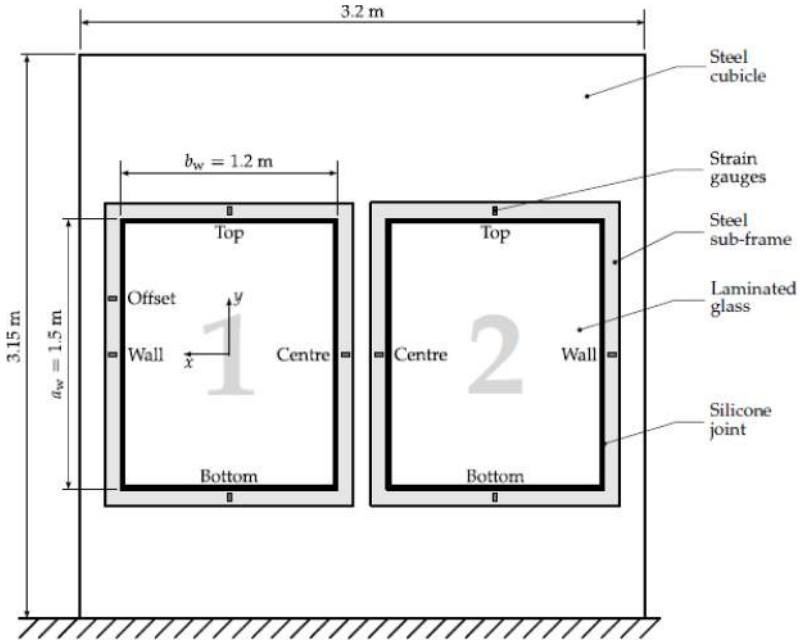

Fig. 12. Full pane test setup completed by Hooper [5].

strain rate to be derived. Strain gauges were also fitted to the frames to measure edge reaction forces. The test setup adopted by Hooper [5] is presented in Fig. 12.

This same arrangement was replicated in LS-Dyna. The test condition simulated was a 30 kg TNT equivalent charge at 16 metre and 14 metre standoff distance, corresponding to Hooper's Tests 3 and 4 respectively. The laminate construction used for Test 3 and 4 was a single layer of PVB (1.52 mm) between two 3 mm annealed glass plies. While MAT_1 Elastic was used in the TCT finite element model to represent the glass, the glass material model in that study did not have an impact on the output as the aim was to isolate the adhesion from the glass and PVB to develop a separate adhesion model in LS-Dyna. Whereas in a full-scale blast test, the softening of the glass post fracture impacts the strength and the displacement shape of the LSG, therefore the glass was modelled using thick shells with a material model that separates the damage between compression and tension (MAT_280). The PVB interlayer was modelled using fully integrated 8-noded quadratic elements with 5 mm x 5 mm edge lengths (aspect ratio 1-5). A mesh sensitivity study was completed, where the aspect ratio was varied between 1-5, 1-3, and 1-1. The difference in peak displacement and edge reactions was negligible, however the overall run-times for the analysis increased exponentially from 1 - 5 to 1-1. Therefore, an aspect ratio of 1-5 was used in the validation. The adhesion was modelled using the same element formulation as in the TCT tests and with the parameters from Table 4. The simulation model developed to replicate the full pane testing is shown in Fig. 13.

Table 6 lists the parameters for the glass material model. Element deletion was not implemented in the model as the glass does have a limited residual capacity, particularly in compression or in bending, that is paramount to the modelling of post crack performance and predicting the deformed shape of the panel. The softening value applied to the model is 0.2 of the stiffness after failure and 0.15 for the stress after failure, therefore the elastic stiffness at failure is reduced to 20% and the stress is reduced to 15% of its capacity at failure. As there is limited data on the stiffness of laminated glass post fracture, these values have been chosen through a parametric study to meet the maximum displacements and deflected shape of the full pane tests. The Rankine stress criterion was used, where the principal stresses are bound by the tensile strength (*ft*) and compressive strength (*fc*). In the development of cracks for MAT_280, a crack occurs perpendicular to the maximum principal stress direction as soon as tensile failure occurs. The tensile scale factor was set to 2.0 after a sensitivity study was conducted in which values from 1 to 5 did not have a significant impact on the overall performance of the LSG in the blast tests. Values greater than 1 are recommended by LSTC to capture high impact loading conditions by LSTC [31].

Table 6
Material properties for annealed glass (MAT_280_GLASS).

	Tensile Strength *ft*	Compression Strength *fc*	Stiffness reduced to% of the elastic stiffness at failure	Stress is reduced to % of failure stress at failure	Tensile Scale Factor
Value	80 MPa	1000 MPa	20	15	2

For the purposes of this investigation, the structural silicone bite was assumed to be of sufficient depth that it would not fail during inward loading as indicated by the test results obtained by Hooper [5]. It is included to simulate the flexibility of the glass edge support. As such, the connection between the inner lite and silicone was meshed in. The silicone was modelled using MAT_24_Piecewise_Linear_Plasticity using information from the product data sheet DOW 995 [32]. MAT_24 is an elasto-plastic material with an arbitrary stress-strain curve. Silicone material details are presented in Table 7.

Blast loading of the pane was replicated using a *LOAD_SEGMENT approach to the external face of the outer lite. With the*LOAD_SEGMENT approach, the *DEFINE_CURVE function was used in which the pressure time history values obtained during the physical experimentation are inputted and applies the load directly to face of the pane. The charge shape in test 3 and test 4 was a rectangular cuboid formed by joining two 12.8 kg C4 charges together to make a total C4 charge of 25.6 kg (taken to be equivalent to 30 kg of TNT). When comparing this to the pressure loads from a spherical 30 kg TNT charge, there are multiple potential discrepancies arising both from the effects of charge shape and the different detonation and afterburn behaviour of the two explosive types. To achieve consistency with the tested configuration, this paper has used the peak reflected overpressure and reflected maximum impulse registered from the experimental data, allowing direct comparison with the test results. Table 8 lists the reflected peak overpressure and reflected maximum impulse.

As seen in Fig. 14, both numerical models predict the midspan displacement of the panes up to the point of maximum displacement. While the model is shown to over predict the maximum displacement for

Table 7
Silicone Details.

	Density	Ultimate Elongation	Ultimate Tensile Strength
Value	1.1 g/cm^3	5.25	1.17 MPa

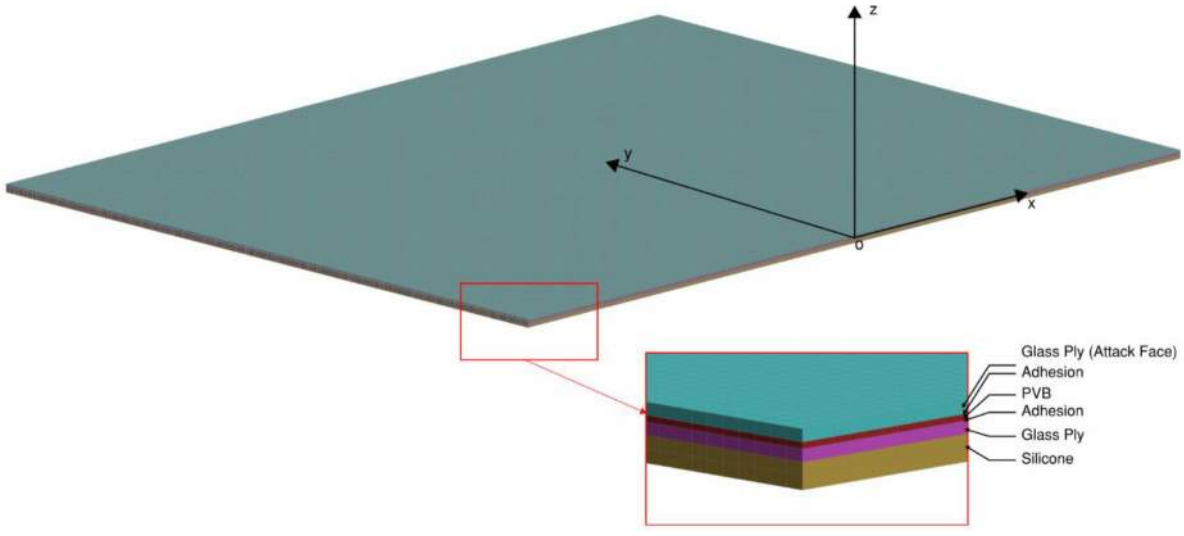

Fig. 13. Makeup of the model with coordinate system.

Table 8
Reflected peak overpressure and reflected maximum impulse.

Test No.	Mass of charge TNT Equivalent (kg)	Standoff (m)	Reflected peak overpressure (kPa)	Reflected maximum impulse (kPa-ms)
Test 3	30	16	132	413
Test 4	30	14	152	461

Test 3, it appears to be under predicting the displacement in Test 4. The difference between peak displacement for Test 4 (30 kg @ 14 m) and the simulation is less than 10%, with the simulation registering a mid-span displacement of 244 mm compared to 266 mm. The model also appears to predict the time of maximum displacement approximately 2 ms behind the maximum displacement in Test 4. For Test 3 (30 kg @ 16 m) and Test 4 (30 kg @ 14 m), joint failure occurred at 16 ms and 19 ms respectively. Hooper notes that during Test 4 (30 kg @ 14 m) the silicone joint failed on all 4 edges and there was a significant inward displacement with the pane impacting the screen protecting the cameras. This led to the displacement of the pane registering a more linear shape in the test. The S-shape shown in the simulation is considered more likely result for a pane with a sufficient retention system. To develop materials specifically for the laminated glass, joint failure was not permitted in the analysis, and therefore detachment of the pane due to cohesive failure in the joint is not witnessed in the simulation. The simulation is compared against the data captured by Hooper [5] pre joint failure, as the data post joint failure is limited during the test.

A further comparison of displaced shapes from Hooper's tests versus the numerical simulation is provided in Fig. 15 for Test 3 (30 kg @ 16 m) and Fig. 16 for Test 4 (30 kg @ 14 m). The peak displacement is within 10% for both tests when comparing the model, demonstrating the applicability of the model for different standoffs. When comparing the overall shape, the simulation exhibits similarities with the tests up to approximately 8 ms. Past this point the centre pane begins to fracture, reducing the glass stiffness and resulting in a displacement shape with a sharper peak.

In undertaking a qualitative comparison of the post-test crack pattern and the output in the simulation, both results demonstrate a heavily cracked LSG as shown in Fig. 17. The pink colour (Value=2) represents 2 cracks in the LSG for each element and the yellow contour (Value =1) is 1 crack for each element.

The short and long glass edge out of plane reaction forces from the simulation are also shown in Fig. 18 for Test 3 (30 kg @ 16 m). When compared to outputs from Wingard PE, an industry accepted analytical tool for assessing a window's response to explosions, the out of plane forces appear conservative with the peak force 15% greater for the long edge and 27% for the shorter edge. This could be due to Wingard PE using a different PVB type, in which case deviation would be expected. This could also be due to the simplified edge condition and the material model used for the silicone material in the engineering model. Further work is required to develop a silicone model for blast modelling applications. Nonetheless, the higher magnitude forces would lead to a somewhat more conservative sizing of silicone bites and framing for façade designers and therefore considered appropriate.

The model resultant reaction forces for the long edge were also compared to the resultant reaction forces outputted post fracture for test 3 (30 kg @ 16 m) by Hooper et al. [33] in Fig. 19. The test results pre fracture (before 4 ms) were not captured in the test data output, and therefore reaction forces pre fracture in the engineering model output are omitted in Fig. 19. When comparing the post fracture reaction forces for the long edge, the initial peak in the engineering model is significantly less than the test initial peak post fracture (43% difference). The secondary peak (predominantly in-plane loading) occurs at 12 ms for the model output and is delayed by 2 ms when compared to the test, however the peak forces at 12 ms are within 5% of the test peak reaction force. Post fracture, the overall shape of the force-time history graph from 6 ms to 16 ms aligns with the test output.

Furthermore, the out-of-plane reaction forces for the model were compared with the 'force-mid span displacement' plots developed in Del Linz [24]. Del Linz [24] using the test data from Hooper [5] plotted the force-mid-span displacement for both pre fracture and post fracture. When comparing the model to these plots, the peaks for both pre fracture and post fracture align well for the mid-span displacement. The initial peak force of the model over predicts when compared to the Del Linz [24] plot, however as shown in Fig. 20, this could be because of the limited data captured pre fracture in Hooper [5]. Additionally, the aim of the model was to develop a methodology to represent the laminated

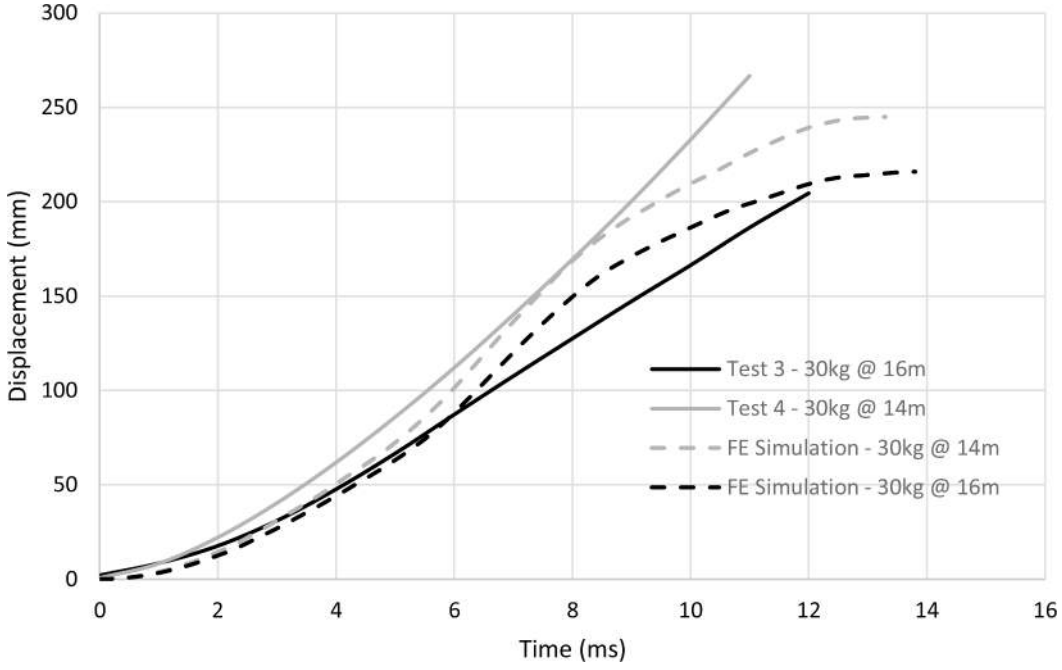

Fig. 14. Comparison of Mid-Span Displacement.

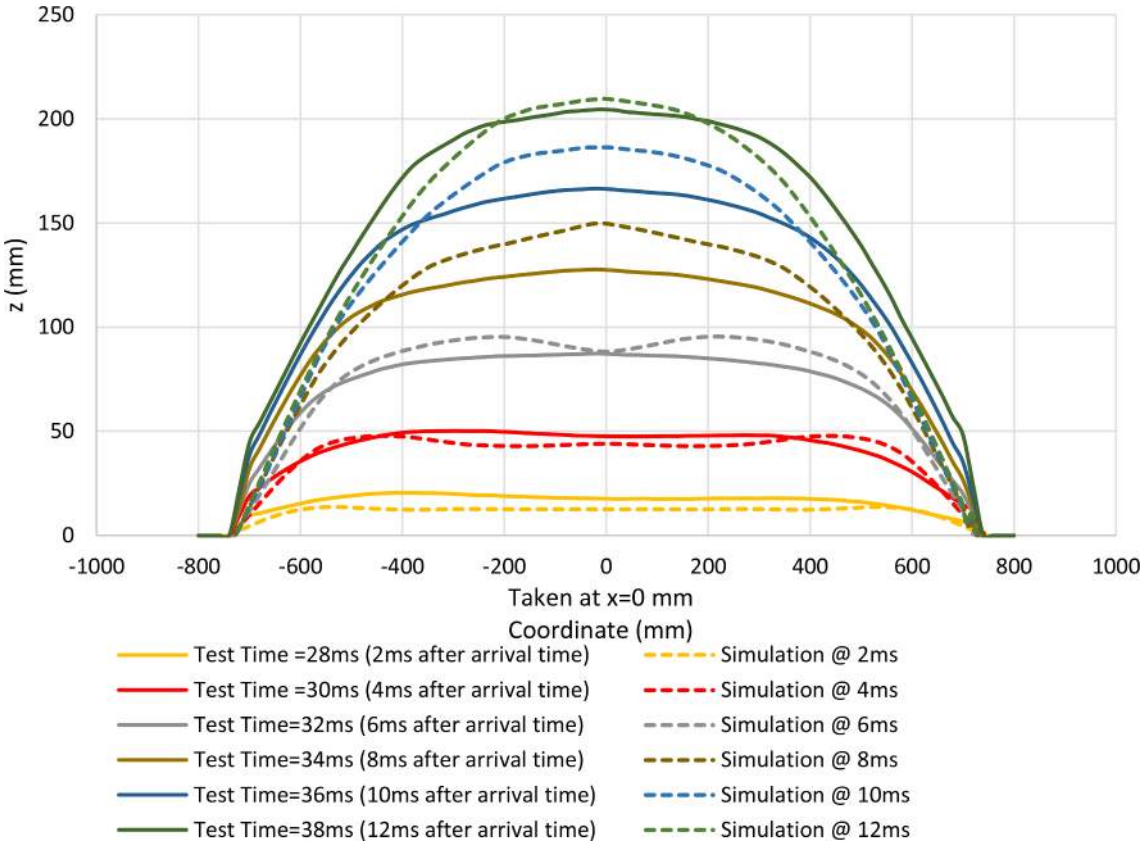

Fig. 15. Contour Plot Comparison for Test 3 (30 kg @ 16 m).

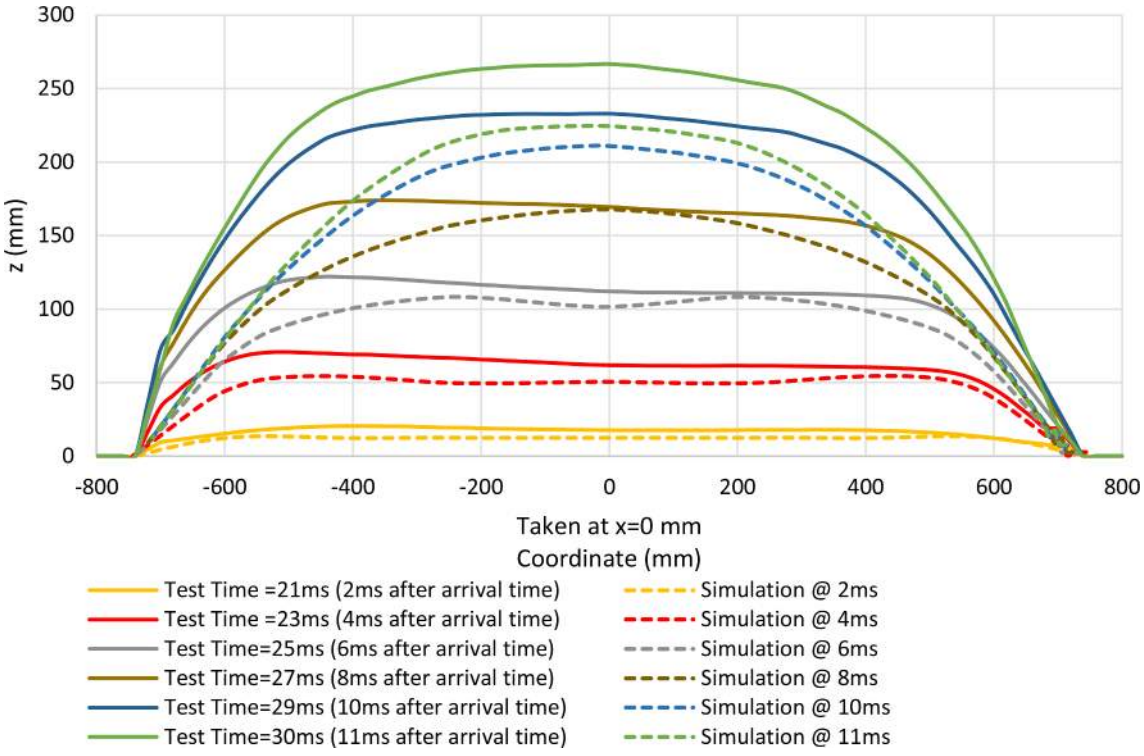

Fig. 16. Contour Plot Comparison for Test 4 (30 kg @ 14 m).

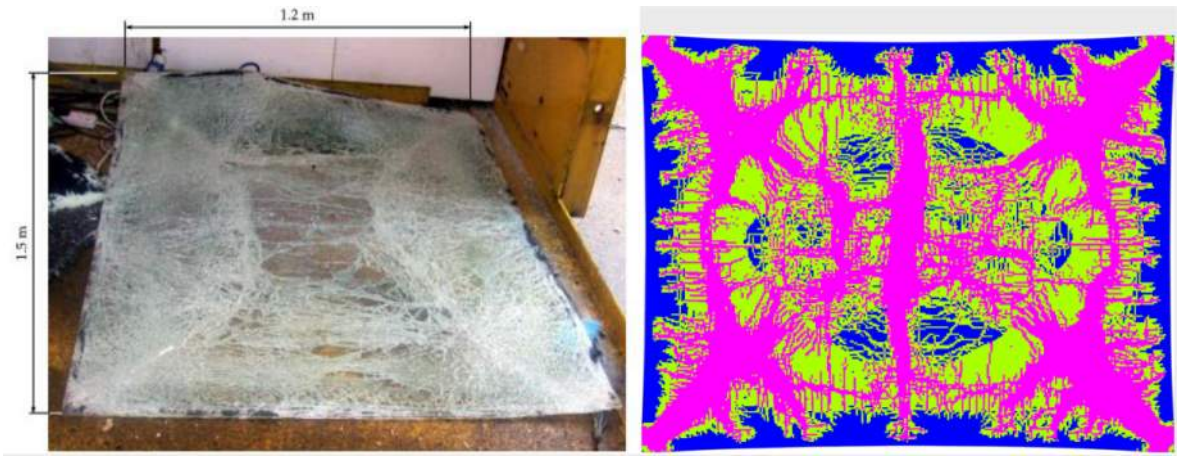

Fig. 17. Comparison of crack pattern between test and simulation.

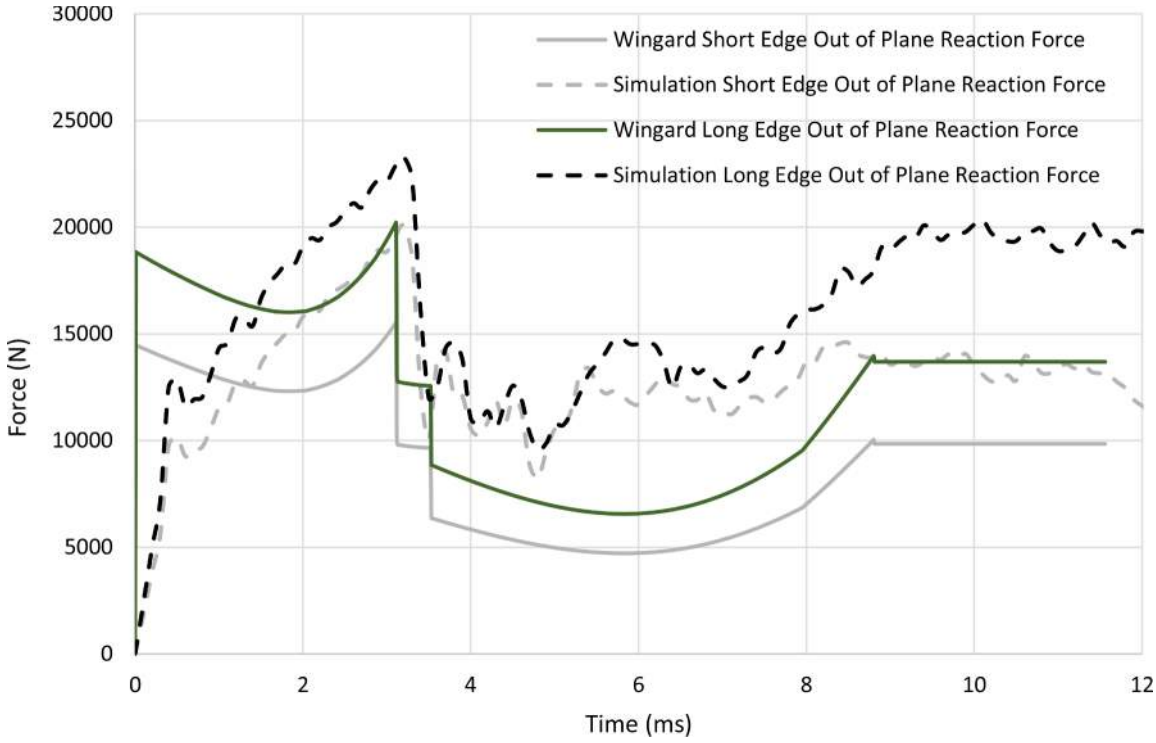

Fig. 18. Out of plane edge reaction comparison between the model and Wingard output for test 3 (30 kg at 16 m).

glass in LS-Dyna and isolate it from the silicone bite. The simplified representation of the silicone bite may be leading to the model over predicting the out-of-plane forces when compared to the test output.

12. FEA model of varying adhesion level

Hooper [5] undertook tests using Saflex RB41, a PVB interlayer with a medium adhesion grade. Cohesive element material properties for other adhesion levels are, however, not well specified in the literature. Elzere [26] has provided test results for low, medium and high adhesion properties at a rate of 1 m/s. In this study, an increase in delamination energy of 150% was found between medium and low adhesion and 170% increase between medium and high adhesion. However, the type of PVB was not specified, and this has an effect on the energy required to delaminate the sample. Sha et al. [12] provided both peak delamination stress and delamination energy values for Saflex RB41 PVB with results indicating that the peak delamination stress identical for both high and medium adhesion. In this study, it was found that there was a 50% increase in delamination energy between low and medium adhesion and a 91% increase between medium and high adhesion.

Using the authors' developed TCT FEA model, peak delamination stress and delamination energy were varied in the simulation to develop an understanding of how varying adhesion levels affect forces and stresses in the PVB material. The indicative values in Table 9 for low and high adhesion are based on the ratios for low-medium and medium-high for Saflex RB41 in Sha et al. [12]. Fig. 21 compares the force with varying displacement for the three adhesion types and Fig. 22 shows the stress distribution in the PVB. Results indicate that a higher adhesion level creates a higher stress in the PVB, likely due to the test requiring more energy to delaminate the interlayer from the glass. Fig. 23 provides a comparison of the edge reactions for the three adhesion levels. The results indicate that there is negligible change in the peak force between the three adhesion types, despite the change in peak delamination stress and delamination energy. Fig. 24 provides a comparison of the crack

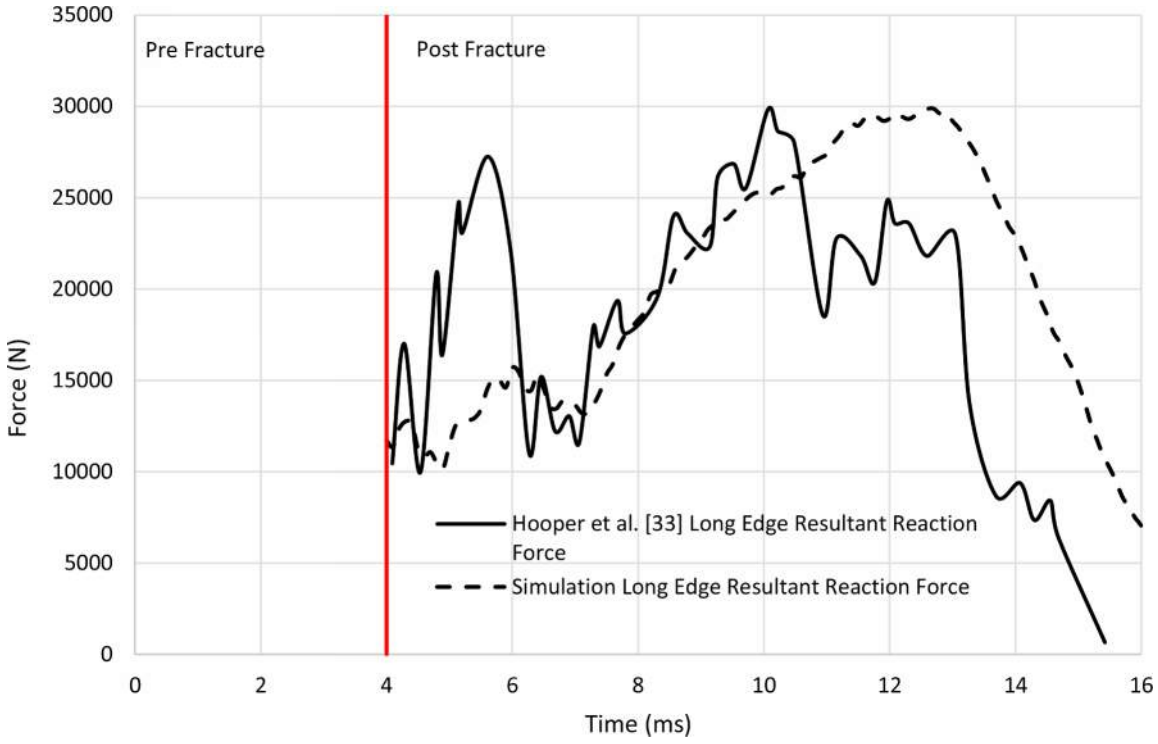

Fig. 19. Total reaction force comparison between the model and the blast test completed in Hooper [34] for Test 3 (30 kg @ 16 m).

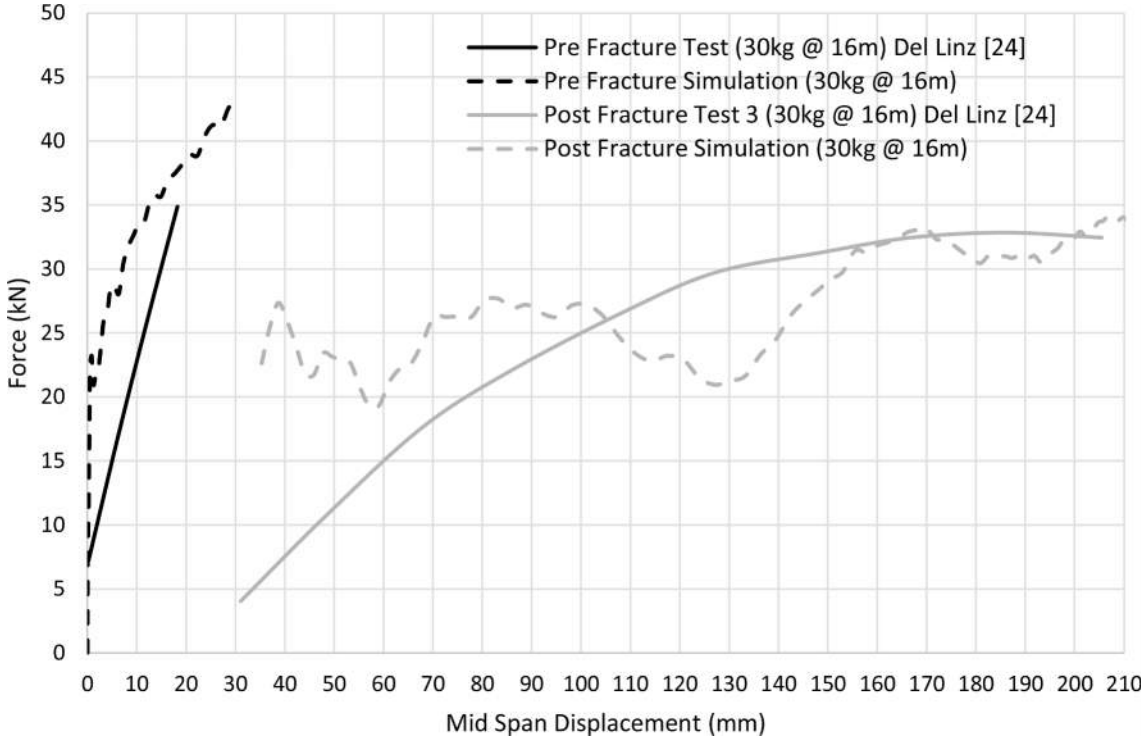

Fig. 20. Pre-Fracture and Post Fracture Force-Central Deflection Comparison between the Model and Del Linz Test Data [24].

Table 9
Values for varying adhesion levels.

Parameter	Low	Medium	High
σ_{-max} (MPa)	1.14	1.8	1.8
G (J/m^2)	2025	3000	5750

pattern between the three adhesion levels. Results indicate that a higher adhesion will increase cracking in the glass pane for the attack face (front pane) however for the rear pane less cracking was witnessed in high adhesion. When mid span displacement is compared in Fig. 25, there are small differences observed between peak displacement for the three adhesion levels. While medium adhesion and high adhesion have

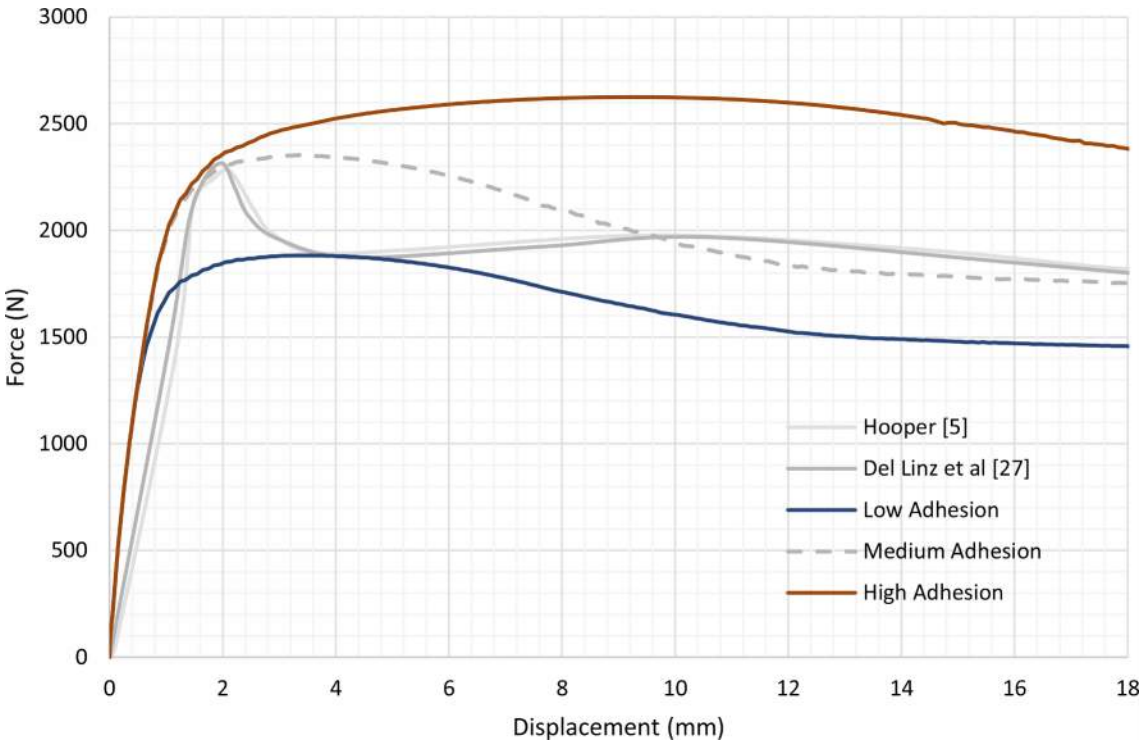

Fig. 21. Comparison with Experimental Test for results of the Through Cracked Test at 1 m/s for low, medium and high adhesion.

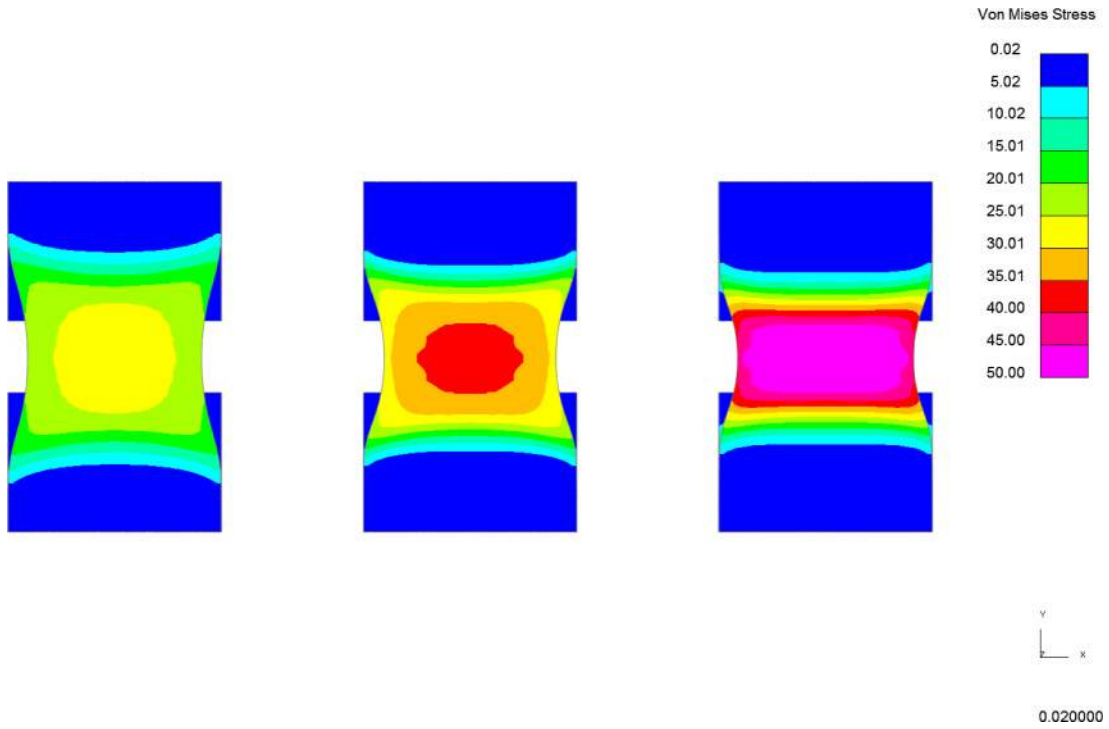

Fig. 22. Comparison of stress in the PVB between Low Adhesion (left) Medium Adhesion (middle) and High Adhesion (right).

an identical peak delamination stress, the larger delamination energy for the high adhesion appears to increase the peak mid span displacement by approximately 6 mm. With attack face (front pane) cracking predominantly increased for higher adhesion, the authors hypothesize that this provides the PVB with more area to elongate between the fragments, resulting in the higher mid span displacement. A comparison of the percentage of the pane cracked and uncracked for the varying adhesion levels is provided in Table 10.

It is observed that there is a larger difference in the percentage of cracking between the front pane and rear panes for low adhesion compared to high adhesion. This suggests high adhesion may have a more symmetric crack pattern. A symmetric crack pattern may have been the contributing factor in the increase in mid-span displacement seen in Fig. 25 for high adhesion. The authors hypothesize that an

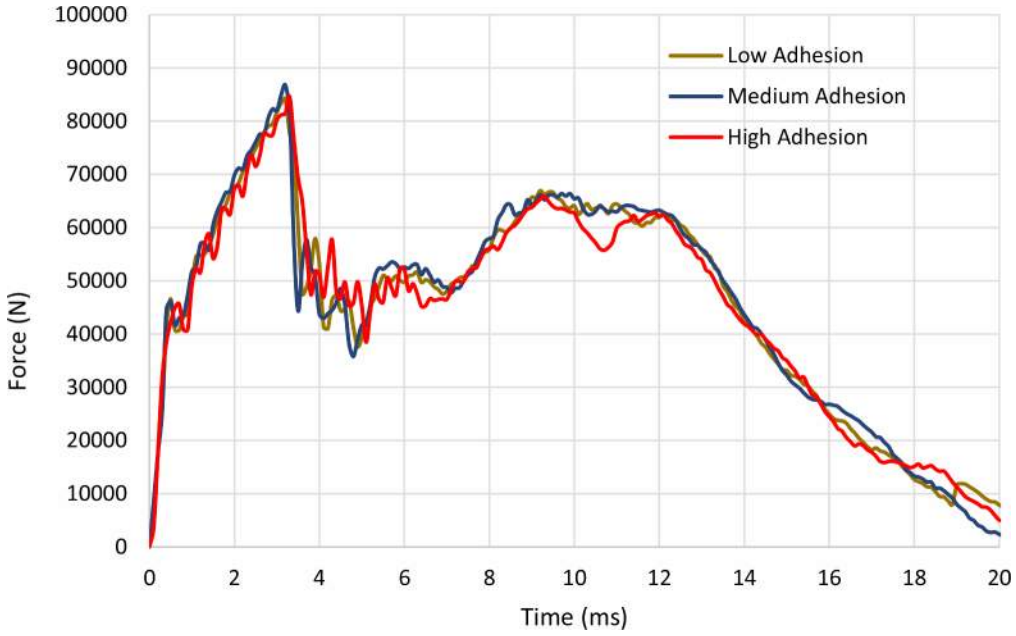

Fig. 23. Comparison of Total Edge Reactions for different adhesion levels.

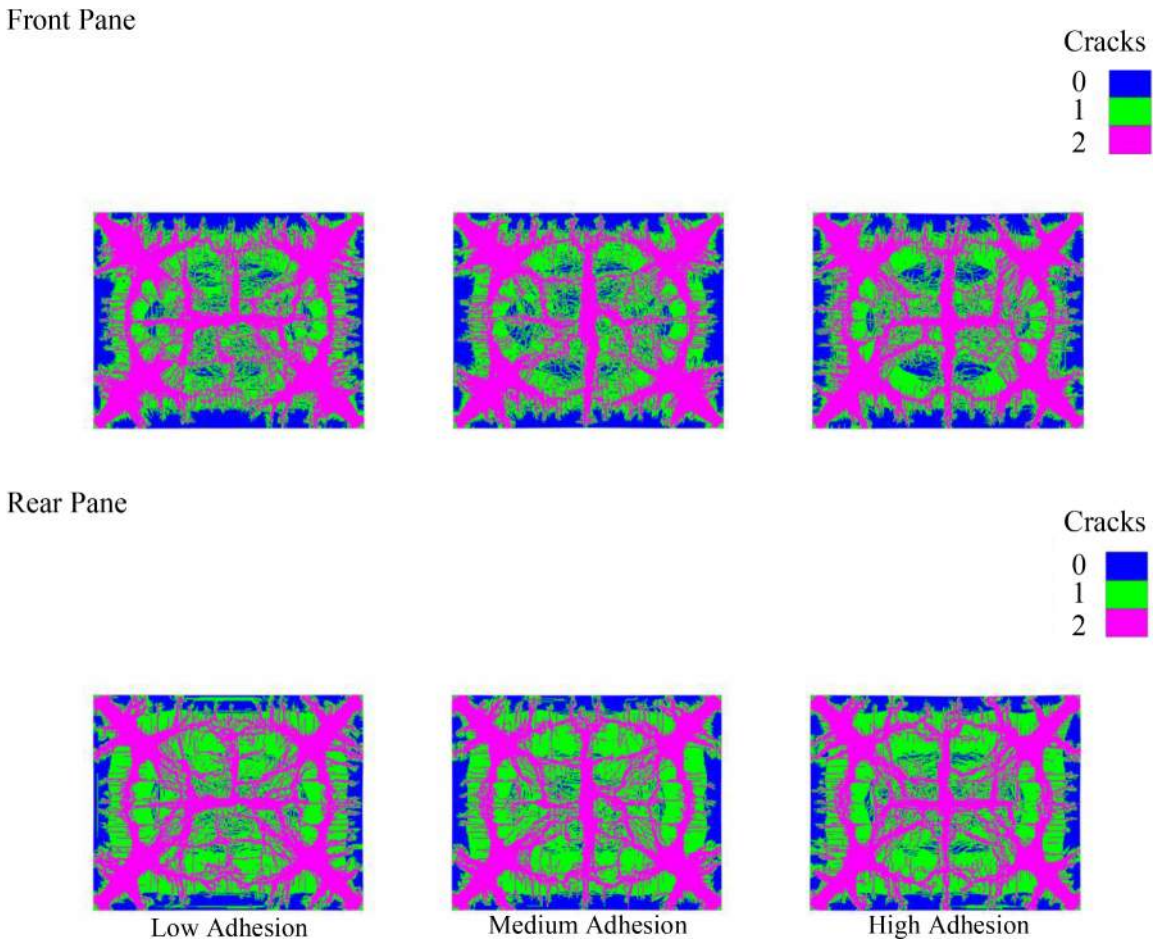

Fig. 24. Variation in Crack Pattern with Adhesion Level for Front Glass (Top/Attack Face) and Rear Glass (Bottom).

asymmetric pattern can restrict the PVB from stretching, compared to a cracking pattern where the cracks line up in the rear and front pane.

Table 11 compares cracking percentage in the centre of the rear pane with different adhesion levels (for a 500 mm x 400 mm rectangular section). As the centre of the pane is where the largest displacements occur, an increase in cracking percentage may result in further

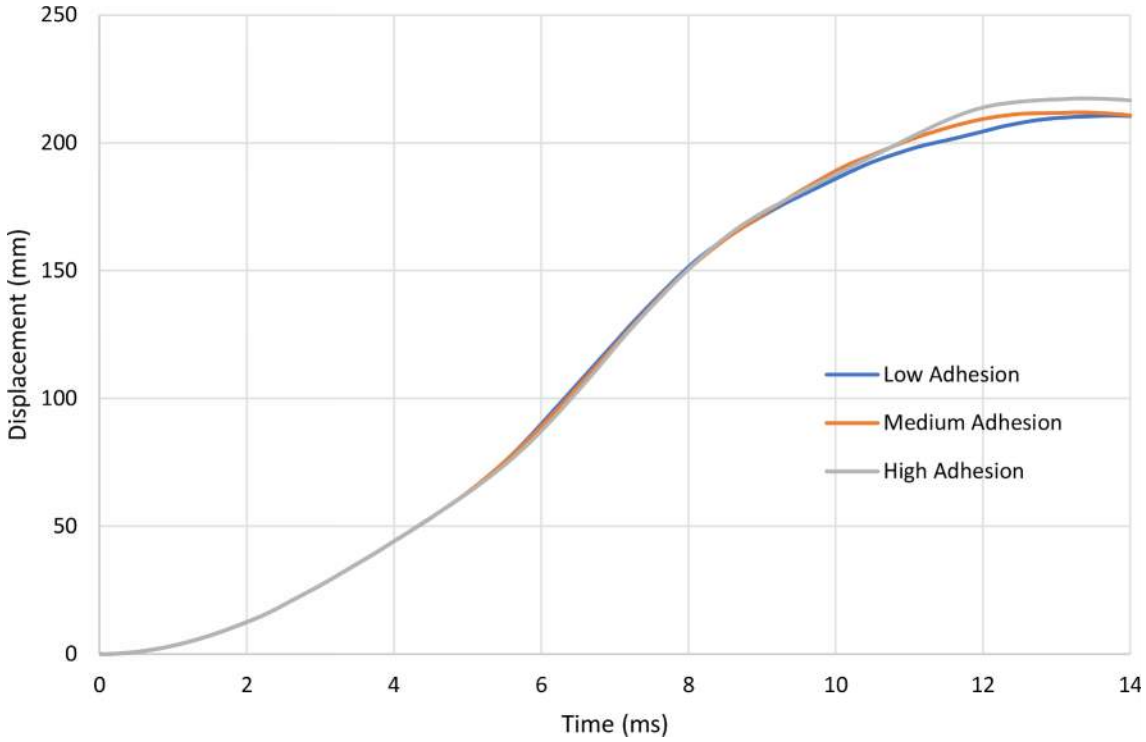

Fig. 25. Comparison of Mid Span Displacement for Varying Adhesion Levels.

Table 10
Percentage of elements uncracked with 1 crack and with 2 or more cracks.

	Glass Top (Front Pane)		Glass Bottom (Rear Pane)	
	Uncracked (%)	Cracked (%)	Uncracked (%)	Cracked (%)
Low Adhesion	35.6	64.4	29.25	70.75
Medium Adhesion	37.09	62.9	30.84	69.16
High Adhesion	36.58	63.42	32.59	67.41

Table 11
Rear Panel Cracking in the Centre of the Pane.

	Rear Pane (Centre of Pane 500 mm x 400 mm Rectangular Section)		
	Uncracked (%)	1 Crack (%)	2 or more Cracks (%)
Low Adhesion	21.99	39.79	38.22
Medium Adhesion	18.73	41.27	40
High Adhesion	16.51	42.34	41.15

fragments being jettisoned off the rear of the pane. As higher adhesion levels are seen to have a higher percentage of cracking in this area, this may suggest increases in adhesion could potentially increase the anticipated fragmentation hazard.

13. Discussion

13.1. Model comparison

A single overall curve fit was selected to reduce the variability when conducting correlation tests for PVB adhesion and to provide simplicity in running further validation studies. The material model adopted in this study demonstrated good correlation to tests 3 & 4 completed by Hooper [5] up to an actuator arm speed of 5 m/s (c.60s^{-1}), particularly between strains of 0.3 to 0.6. It is noted that the material model appears to under predict the stress at strain rates higher than 0.6. This is a result of the PVB 'dogbone' sample undergoing large stretching, resulting in a softening of the material. Based on the completed simulations of the glass and adhesion, the PVB strain however does not reach levels during blast tests that are sufficient to negatively affect the validity of the simulation.

Whilst strain rate specific curve fits are found to demonstrate better correlation for the PVB when compared to the single overall curve fit, to use a strain rate specific curve fit requires an understanding of the expected strain rate of the LSG prior to simulation. Del Linz et al. [17] suggested a PVB material model should ideally represent the entire range of rates, as strain rate is difficult to predict. Additionally, under blast loads, strain rates have been observed to vary over a pane, with some regions experiencing higher rates than others. Various authors have hence elected to represent the PVB response using low and high strain rate curves such as Del Linz et al. [17]. While this reduces the requirement for a material model to represent the PVB for each strain rate, it still requires the need for two material models for the two strain rates and two separate material models for adhesion to fit the PVB. It is found the overall curve fit is the most reasonable in correlating to the tensile tests, the most practical for developing the adhesion material properties and, subsequently to simulate full LSG panes subjected to blast loads.

The authors have developed a medium level adhesion material model based on the through cracked tensile tests completed by Del Linz et al. [27], and Hooper [5]. The results of the material model demonstrate correlation with the plateau force and the peak load. It was not possible to replicate the rapid drop in observed peak tensile force to the steady state plateau level. The authors propose that this is attributed to the force required to initiate delamination being larger than that required to maintain a delamination front. In this respect, there are similarities with mechanical fracture mechanisms. This is supported by Samieian et al. [6] who proposed that the bond fracture toughness is loading rate dependant, up to a limit of 20/s and any further increase in loading rate did not result in a change in facture toughness. In the peeling of flexible laminates, Samieian et al. [6] stated that the fracture toughness is a factor of the local plastic or viscoelastic energy dissipation in the zone ahead of the peeling front. Nonetheless, the model is able to

demonstrate reasonable correlation of the plateau force and overall work done, which are considered the important parameters for simulating full panes subjected to blast loads.

Finally, the full pane model was compared to the full-scale blast tests completed by Hooper [5]. Of significance is the utilisation of a glass material that maintains load carrying capacity post fracture. Galuppi & Royer-Carfagni [34] stated that the residual strength of the laminate is related to the size of the glass fragment. Though with limited post fracture values available, the assessment completed within this study were tailored to meet the overall shape and peak of Hooper's test 3 (30 kg @ 16 m). These values were than applied to Hooper's Test 4. The assessment demonstrated reasonable comparison to the midspan displacement within 10% for Test 3 and 15% for Test 4. In addition, the overall deformed shape in the simulation showed a similar shape up to approximately 8 ms for both tests.

The glass edge reactions from the simulation were compared to estimated edge reactions in Wingard PE and Del Linz [24] and the test 3 long edge reaction output in Hooper [33]. The overall curve shape curve is similar in response, and peak forces are similar. It is noted that the PVB is not specified in Wingard PE and, if a different PVB material was used a deviation in the overall result would be expected. A difference in the initial peak force ($t = 5$ ms) outputted in the test data by Hooper [33] is witnessed when comparing to the model output post fracture. It is hypothesized that as the aluminium frame is not modelled, the initial peak force post fracture is higher in the test as a result of the frame undergoing strain hardening as it begins to deform and as the in-plane loading grows to become the predominant force vector. However, even though the secondary peak force is delayed, the peak force (predominantly in-plane forces) is similar in magnitude, and the overall shape of the curve aligns well from 6 ms-16 ms. Finally, when comparing the out-of-plane reaction forces from Del Linz [24] and the model output, the forces align well with the mid-span displacement. The model overpredicts the initial out-of-plane force pre fracture, however, is within a similar magnitude post fracture. It is recognised that a more detailed silicone material is required for blast simulation. Nevertheless, the reactions in the model are within the approximate magnitudes for the comparison of adhesion levels and its impact on edge reactions post fracture.

13.2. Adhesion comparison

Following the calibration of the medium level adhesion material model, a further assessment on the effects of low and high adhesion was investigated. Table 1 demonstrates a wide range of values in literature for adhesion levels. Elzere [26] provided peak delamination stress and delamination energy values for low, medium and high adhesion based on very low actuator arm speeds and demonstrated the ratio differences between medium and high to be in excess of 150%, and between low and medium to be approximately 150%. It should be noted, however, that the adhesion properties developed for low, medium and high by Elzere [26] were at varying strain rates, lower than what is commonly seen in full-scale blast tests. Sha et al. [12] also conducted a variety of through cracked tensile tests with Saflex RB41 and provided peak delamination stress and delamination energy values for low, medium and high adhesion at low strain rates. This demonstrated a 50% increase in delamination energy between low and medium adhesion and a 90% increase in delamination energy between medium and high adhesion. These values provided by Sha et al. [12] were therefore chosen to represent low and high adhesion in this study.

The authors have developed the model with the intention to isolate the effect of adhesion from PVB performance using 'gap' elements. This is of particular relevance to façade system designers as higher adhesion levels are commonly adopted to reduce the potential for visual defects in glass. Using the full-scale blast test comparison, the out-of-plane glass edge reactions were assessed demonstrating minimal variation on the peak force and force time history graph. This study is considered to be important because an increase in loads could result in the failure of the retention system including the structural silicone bite, the size of which is often determined using historic testing or based on a PVB interlayer with a medium adhesion level. Mid span displacement was also compared for all three adhesion levels. It was found that a more cracked LSG led to a higher mid span displacement. This is attributed to more cracking for high adhesion, allowing the PVB to elongate further. Additional cracking could bring on more debris being jettisoned off the pane potentially registering a worse GSA [35] performance condition and failing the pane. As the GSA fragment measurement approach is used by designers as a method of demonstrating compliance with blast façade design objectives, further tests should be undertaken to investigate whether adhesion levels influence the GSA [35] performance condition of LSG.

14. Conclusion

Using LS-Dyna, PVB tensile tests were replicated for actuator arm speeds between 0.1 m/s to 5 m/s to investigate the influence of PVB-glass adhesion in LSG at high strain rates. A single material model was used to represent the PVB for this strain range that demonstrated reasonable correlation with the test results sourced from literature. Above the strain of 0.6, the model begins to under predict stress due to numerical issues associated with over-stretched elements. However, based on the completed simulations of the glass and adhesion, the PVB strain typically does not reach levels during blast tests that are sufficient to negatively affect the validity of the simulation.

Utilising the results from PVB correlation, a through cracked tensile test was then replicated and an adhesion material model was calibrated against testing data for a PVB interlayer with medium adhesion properties (Saflex RB41). The modelling results demonstrated a similar peak force and work done to the physical test results. Finally, the full pane model was compared against two blast tests and showed reasonable correlation of mid-span displacement, which was within 15% of the test values.

Representative values for low and high adhesion properties were presented based on ratios provided in literature. Through simulation, it was found that the transition from a low to high adhesion level does not significantly affect the displacement or the glass edge reactions of the pane. It did appear however that a higher adhesion level can increase cracking, particularly mid-pane on the rear side of the glass pane. Higher levels of cracking could give rise to a lower bond area, which may increase debris being projected from the pane. As the proposed model is not able to capture the trajectory of fragments discarded off the pane, it is recommended that further full-scale tests with varying adhesion levels are conducted to identify whether the fracture pattern can negatively impact the GSA [35] performance condition used in design of LSG.

Data availability

Data will be made available on request.

CRediT authorship contribution statement

D. Aggromito: Validation, Methodology, Writing – original draft, Data curation, Formal analysis. **L. Pascoe:** Writing – review & editing, Conceptualization, Methodology, Supervision. **J. Klimenko:** Writing – review & editing, Data curation. **J. Farley:** Validation, Writing – review & editing. **M. Tatarsky:** Formal analysis, Validation. **W. Wholey:** Conceptualization, Methodology, Writing – review & editing.

Declaration of Competing Interest

The authors declare that they have no known competing financial interests or personal relationships that could have appeared to influence the work reported in this paper.

Data Availability

Data will be made available on request.

References

[1] American Society of Civil Engineers. (2011). Blast Protection of Buildings.
[2] SAFE/SSG. Glazing hazard guide, cubicle stand-offs, tables & charts. London: Explosive Protection; 1997. SSG/EP/4/97.
[3] Technical Applied Research Inc. (2005). Window Glazing Analysis Response & Design (WINGARD).
[4] Morrison C. PhD Thesis. Cranfield University; 2007.
[5] Hooper P. PhD Thesis. Imperial College London; 2011.
[6] Samieian M, Cormie D, Smith D, Wholey W, Blackman BRK, Dear JP, Hooper PA. On the bonding between glass and PVB in laminated glass. Eng Fract Mech 2019; 214:504–19.
[7] Alter C, Kolling S, Schneider J. A New Failure Criterion for Laminated Safety Glass. In: 11th European LS-DYNA Conference; 2017.
[8] Centre for Protection of National Infrastructure. Laminated glass recommended PVB interlayers for blast requirements, interim guidance, version 1. 2020. Retrieved at, https://www.cpni.gov.uk/system/files/documents/66/bd/GN%20Interlayers%20for%20Blast%20requirements%20-%20FINAL.pdf.
[9] Butchart C, Overend M. *Delamination in fractured laminated glass* [Paper presentation]. In: In engineered transparency. International Conference at glasstec; 2012.
[10] Xu J, Li Y, Liu B, Zhu M. Experimental investigation on constitutive behaviour of PVB under impact loading. Int J Impact Eng 2011;38:106–14.
[11] Zhang X, Hao H, Shi Y, Cui J. The mechanical properties of Polyvinyl Butyral (PVB) at high strain rates. Construct Build Mater 2015;93:404–15.
[12] Sha Y, Hui CY, Kramer EJ, Garrett PD, Knapczyk JW. Analysis of adhesion and interface debonding in laminated safety glass. J Adhes Sci Technol 1997;11(1): 49–63.
[13] Butchart C, Overend M. *Influence of moisture on the post-fracture performance of laminated glass* [Paper presentation]. In: Glass Performance Days Conference; 2013.
[14] Andreozzi L, Bati SB, Fagone M, Ranocchiai G, Zulli F. Dynamic torsion tests to characterize the thermo-viscoelastic properties of polymeric interlayers for laminated glass. Construct Build Mater 2014;65:1–13.
[15] Suwen C, Xing X, Xiqiang W. The mechanical behaviour of polyvinyl butyral at intermediate strain rates and different temperatures. Construct Build Mater 2018; 182:66–79.
[16] Klock D. Ph.D. Thesis. Université de Haute Alsace; 1989.
[17] Del Linz P, Wang Y, Hooper PA, Arora H, Smith D, Pascoe L, Cormie D, Blackman BRK, Dear JP. Determining material response for polyvinyl butyral (PVB) in blast loading situations. Exp Mech 2016.
[18] Keller U, Mortelmans H. *Adhesion in laminated safety glass – what makes it work?* [Paper presentation]. In: Glass Processing Days Conference; 1999.
[19] Samieian M. PhD Thesis. Imperial College London; 2018.
[20] Descamps P, Durbecq S, Hayez V, Chabih M, Van Wessenhove G. *Dimensioning silicone joints used in bomb blast resistant façade systems* [Paper Presentation]. In: Challenging Glass 6 – Conference on Architectural and Structural Applications of Glass Louter; 2018. *Bos, Belis, Veer, Nijsse (Eds.)*.
[21] Trosifol K. Pummel Test Standards. 2017.
[22] Jagota A, Bennison SJ, Smith CA. Analysis of a compressive shear test for adhesion between elastomeric polymers and rigid substrates. Int J Fract 2000;(104):105–30.
[23] Palfrene J, Van Dam S, Van Paepegem W. Numerical analysis of the peel test for characterisation of interfacial debonding in laminated glass. Int J Adhes Adhes 2015;62:146–53.
[24] Del Linz P. PhD Thesis. Imperial College London; 2014.
[25] Muralidhar S, Jagota A, Bennison SJ, Saigal S. Mechanical behaviour in tension of cracked glass bridged by an elastomeric ligament, 48. Acta Metallurgica Inc; 2000. p. 4577–88.
[26] Eziere P. [unpublished thesis]. Universite Pierre et Marie Curie; 2017.
[27] Del Linz P, Hooper PA, Arora H, Wang Y, Smith BBRK, Dear JPP. Delamination properties of laminated glass windows subject to blast loading. Int J Impact Eng 2017;105:39–53.
[28] ISO 16933 (2007). Glass in Building – Explosion-resistant security glazing – Test and classification for arena air-blast loading. First Edition.
[29] ISO 16934 (2007). Glass in Building – Explosion-resistant security glazing – Test and classification by shock-tube loading. First Edition.
[30] Kranzer C, Gurge G, Mayrhoffer C. *Testing of bomb resistant glazing systems. Experimental investigation of the time dependent deflection of blast loaded 7.*5mm *laminated glass*. Glass processing days. 2005.
[31] Livermore Software Technology Corporation. LS-DYNA material manual. USA: Livermore California; 2018.
[32] Dow corning 995 silicone structural glazing sealant technical data sheet form no. 62-1260-01J. The Dow Chemical Company; 2018.
[33] Hooper PA, Sukhram RAM, Blackman BRK, Dear JP. On the blast resistance of laminated glass. Int J Solids Struct 2012;49:899–918.
[34] Galuppi L, Royer-Carfagni G. The post-breakage response of laminated heat-treated glass under in plane and out of plane loading. Composites 2018;147(Part B): 227–39.
[35] General Services Administration Progressive Collapse Analysis and Design Guidelines (2003). United States General Services Administration.